Quantifying the Sources of Forecaster Disagreement

Husang Kim*

November 17, 2026

Abstract

Using a multivariate factor model based on the noisy information framework, this study decomposes forecaster disagreement about real output growth and inflation into three sources: individual anchors, heterogeneous responses to common belief shocks, and idiosyncratic noise shocks. Unconditionally, noise shocks explain a large share of the disagreement, whereas common belief shocks contribute more intermittently and are relevant to the countercyclicality of growth disagreement. Classifying these shocks into supply and demand types highlights the variable-specific nature of disagreement: growth disagreement is shaped primarily by demand-side information, inflation disagreement by supply-side information. It also shows that economic events with observationally similar disagreement patterns mask distinct underlying dynamics.

Keywords: Imperfect Information, Noisy Information, Forecaster Disagreement, Factor Model

JEL Classification: C53, D83, D84, E31, E32, E37

*Department of Economics, The University of Texas at Austin, 2225 Speedway, Austin, TX 78712 (e-mail: hs.kim@utexas.edu). I thank the anonymous referees for comments and feedback. I especially thank Olivier Coibion and Stefano Eusepi for their guidance and support. I am grateful to Saroj Bhattarai, Chris Boehm, Andres Drenik, Andreas Mueller, Ehud Ronn, Daniel Frost, Faheem Gilani, Rikuto Onishi, Hayden Parsley, Zebang Xu, and seminar participants at various venues for helpful comments. I also thank Christiane Baumeister for feedback that led to a substantial improvement of the analysis in this paper.

1 Introduction

Disagreement in expectations has long been a key focus in macroeconomic research. It not only serves as direct empirical evidence against the Full-Information Rational Expectations (FIRE) but also carries significant macroeconomic implications, ranging widely from business cycles (Lorenzoni, 2009; Angeletos and La'O, 2013) and asset pricing (Miller, 1977; Scheinkman and Xiong, 2003) to monetary policy transmission (Falck, Hoffmann, and Hürtgen, 2021) and resource misallocation (Coibion, Gorodnichenko, and Ropele, 2023). Disagreement can arise for several reasons. Agents may possess different information about the state of the economy or different subjective models of understanding the economy. Alternatively, they could be biased in fundamentally different ways, leading to heterogeneous predictions even when they hold the same information and model. This raises several interesting questions: What is the predominant source of observed disagreement? To what extent does each form of heterogeneity contribute to disagreement? Does the contribution of each source vary over time and across variables? Furthermore, does the spike in disagreement typically seen during major economic events share similar underlying dynamics?

This paper addresses these questions by providing a historical decomposition of disagreement in the inflation and output growth forecasts from the Blue Chip Economic Indicators. To this end, I use a factor model of forecasts that can be easily traced back to a standard noisy information model that underpins the diverse models of expectation formation investigated in the literature. Each term in the factor model has a clear interpretation, and together the terms point to three distinct sources of disagreement: individual-specific anchors, heterogeneous responses to common belief shocks, and idiosyncratic noise shocks. The analysis delivers two sets of findings. Conditionally, the drivers of disagreement vary substantially over time and across variables: observationally similar spikes in disagreement conceal distinct underlying dynamics across historical episodes, and the nature of disagreement differs across variables. Unconditionally, noise shocks, and hence information dispersion, constitute the major source of disagreement, accounting for more than half of the observed disagreement on average over the sample period. In comparison, the contribution from individual anchors is non-trivial, consistently around 10-20%, and common belief shocks contribute more intermittently, being relevant to the countercyclicality of growth disagreement. These patterns underscore that, on top of information dispersion, integrating additional sources of heterogeneity into the expectation formation process is important.

More specifically, the analysis begins with a standard noisy information framework that motivates the empirical analysis. The framework is enriched in three dimensions: (i) a multivariate setup with imperfect information, where agents observe noisy signals about

real output growth and inflation; (ii) non-information heterogeneity, such as differences in signal precision and subjective models of the economy; (iii) individual anchors that capture heterogeneity in perceived long-run means.

The model implies an empirically estimable factor model of forecasts, identifying three sources of disagreement. The first source, individual anchors, is represented by individual fixed effects, capturing systematic and time-invariant heterogeneity in the level of forecasts, which mainly reflects differences in perceived long-run means (Setup (iii)). The second source, common belief shocks, is linked to the estimated factors, fostering disagreement by amplifying the differences in individual-specific loadings on the factors (Setup (ii)). Intuitively, the factor loadings are unique to each forecaster due to heterogeneous Kalman gains. As forecasters place different weights (gains) on new information (signals), it amounts to different perceived effects of common belief shocks. The final source, idiosyncratic noise shocks, is encapsulated in each forecaster's residuals. These reflect the *unsystematic and time-varying* heterogeneity among agents, possibly due to the dispersed information across agents from noisy private signals (Setup (i)).

Building on the framework of Juodis and Kučinskas (2023), the estimation result suggests that the noise shocks are identified as the primary source of disagreement. However, the analysis further reveals various dynamics across different economic episodes. Specifically, common belief shocks play a more prominent role during the Gulf War recession and post-pandemic inflation surge episodes, when forecasters interpret the same large disruption differently. Conversely, the contribution of noise shocks was very salient during the Dot-com recession, the Financial Crisis, and the Covid-19 recession, which featured significant real-time and financial uncertainty. This suggests that the significance of each source of heterogeneity varies over time and that the apparent similarity in the fluctuations of disagreement actually masks heterogeneous underlying dynamics.

Furthermore, the common belief shocks and idiosyncratic noise shocks are classified into supply and demand types. This classification offers a parsimonious framework to analyze the sources of disagreement, as the concepts of supply and demand could capture diverse structural disturbances that forecasters may consider in forming beliefs. To achieve this, the paper employs a two-step identification strategy: conventional sign restrictions for common belief shocks (Uhlig, 2005) and higher-order moment conditions for noise shocks (Bekaert, Engstrom, and Ermolov, 2021). The novelty of the paper is that the shocks are *point-identifed*. Crucially, for the common belief shocks, while sign restrictions typically yield only set identification, I utilize the forecaster microdata to achieve *point identification*. Similarly, the reliance on higher-order moments, motivated by pervasive non-Gaussianity in survey data (Bekaert, Engstrom, and Ermolov, 2021), also allows for the *point identification* of

idiosyncratic noise shocks. This paper thus contributes by providing a unified multivariate framework that uniquely achieves point identification for both common and idiosyncratic sources of disagreement.

The identified shocks are further validated through their dynamic effects on macroeconomic expectations. Impulse responses estimated from panel local projections show that the responses of growth, inflation, and interest rate forecasts align with the conventional supply and demand logic. The interest rate forecast, which is not used in the identification, serves as an external check. The exercise also uncovers a behavioral distinction between the common belief and idiosyncratic noise shocks. Expectations respond to common belief shocks in a persistent manner, whereas the effects of noise shocks dissipate within a few months, reinforcing the interpretation of the latter component as transitory noise rather than lasting information heterogeneity.

Classifying shocks into different types offers valuable insights into the multivariate nature of disagreement. The results indicate that real output growth disagreement is primarily driven by demand noise shocks, while inflation disagreement is largely influenced by supply noise shocks. For example, during the post-pandemic inflation surge, inflation disagreement reflected dispersed information about the persistence of supply shocks. This suggests that although information dispersion is the key driver of disagreement, the specific nature of the information that agents disagree on differs across economic variables.

This paper mainly contributes to the macroeconomic literature that investigates the sources of heterogeneous beliefs. Disagreement across agents could arise due to differences in information (Mankiw and Reis, 2002; Woodford, 2003; Coibion and Gorodnichenko, 2012; Coibion and Gorodnichenko, 2015; Angeletos, Huo, and K. A. Sastry, 2021), or from non-information heterogeneity such as different degrees of inattention (Sims, 2003) or subjective models (Bray and Savin, 1986; Marcet and Sargent, 1989; Andre et al., 2022; Crump, Eusepi, and Moench, 2024). Additionally, agents can differ in their long-run priors (Patton and Timmermann, 2010), or deviate from the optimal Bayesian forecast because of heterogeneous objective functions (Capistrán and Timmermann, 2009) or forecasting models (Giacomini, Skreta, and Turen, 2020). This paper contributes by quantifying the relative importance of each channel and providing a comprehensive account of the sources of disagreement in different economic episodes.

The main finding of this paper especially puts emphasis on the theoretical literature that relies on noisy information to investigate the role of heterogeneous beliefs in macroeconomic research. Disagreement due to dispersed information could generate non-fundamental-driven business cycles (Lorenzoni, 2009; Angeletos and La'o, 2010; Angeletos and La'O, 2013). It also has implications for monetary policy (Woodford, 2003; Angeletos and La'o, 2020; Falck,

Hoffmann, and Hürtgen, 2021) and asset pricing (Scheinkman and Xiong, 2003; Carlin, Longstaff, and Matoba, 2014). Despite the widespread use of dispersed information as a modeling device, the extent to which dispersed information caused by noisy signals contributes to disagreement remains an open empirical question. This paper addresses this gap by identifying forecaster-specific noise shocks and quantifying their level of importance in terms of disagreement.

This paper is also related to the voluminous literature that analyzes disagreement among professional forecasters through the lens of imperfect information. The literature has largely focused on finding stylized facts of disagreement that contribute to refining expectation formation models. For example, Andrade and Le Bihan (2013) investigate the information update behavior and disagreement among forecasters, providing an empirical evaluation of inattention models. Andrade, Crump, et al. (2016) offer new stylized facts about the term structure of disagreement and suggest possible modifications of imperfect information models. Dovern (2015) and Rich and Tracy (2021) document heterogeneity and persistence of individual disagreement, which provide a basis for further development of expectation formation models. Lahiri and Sheng (2008) propose a Bayesian learning model to explain the evolution of disagreement over horizons. While these existing studies focused on matching the stylized facts of disagreement observed in the data, this paper takes a step further. It not only points out the overall, *unconditional* source of disagreement but also offers a historical decomposition of disagreement, which pinpoints the source of disagreement *conditional* on each point in time and episode.

The work most closely related to this paper is Herbst and Winkler (2026), who employ a factor model grounded in the noisy information framework to decompose disagreement. In their baseline setup, agents receive noisy signals about aggregate shocks and the disagreement stems from a single source, information dispersion. Relative to their framework, this paper delivers three different sources of disagreement: forecaster-specific anchors, heterogeneous responses to common belief shocks, and idiosyncratic supply and demand noise shocks that are point-identified at the forecaster level. These additional channels turn out to be quantitatively important, with anchors and heterogeneous responses jointly accounting for roughly 30% of observed disagreement. In terms of results, their growth disagreement is mainly supply-driven, unlike in this paper. This may partly reflect their sample period, which includes the 1970s when supply disagreement was most important, as well as the different datasets (quarterly SPF versus monthly Blue Chip) and identification assumptions (Gaussian versus non-Gaussian shocks). For inflation, the GDP deflator disagreement in their paper, the inflation measure used here, is supply-driven, in line with this paper.

Also relevant is Ahn and Farmer (2024), who analyze the term structure of inflation

disagreement. While they focus on the horizon dimension of a univariate expectation, this paper distinguishes itself by focusing on the multivariate dimension of disagreement while utilizing the joint identification of supply and demand drivers of disagreement.

The paper is organized as follows. Section 2 introduces the framework of noisy information and derives a factor model of forecasts. Section 3 discusses the data, estimation, and identification strategy. Section 4 presents the empirical results: the dynamic effects of the identified shocks and the historical decomposition of disagreement. Section 5 provides further discussion and robustness checks. Section 6 concludes.

2 Conceptual Framework

This section begins by introducing an extension of the noisy information model. The goal is to motivate and provide a semi-structural interpretation of the empirical factor model of the forecast.

2.1 Noisy Information Model

In the standard noisy information model (Sims, 2003; Woodford, 2003), agents only have access to contaminated signals of aggregate states. More specifically, consider a vector of N_x target variables ($\mathbf{x}_t$), whose data-generating process (DGP) can be described as follows.

$$\mathbf{x}_t = \boldsymbol{\mu} + \mathbf{A}\left(\mathbf{x}_{t-1} - \boldsymbol{\mu}\right) + \mathbf{B}\boldsymbol{\epsilon}_t \tag{1}$$

In equation (1), $\mathbf{A}$ is an $(N_x \times N_x)$ matrix with all eigenvalues inside the unit circle. $\boldsymbol{\epsilon}_t$ represents a $(N_\epsilon \times 1)$ vector of shocks with mean zero and a covariance matrix denoted as $\boldsymbol{\Sigma}_{\boldsymbol{\epsilon}}$, where the off-diagonal entries are zero. $\mathbf{B}$ is an $(N_x \times N_\epsilon)$ impact matrix loaded on the shocks.

Although the framework in (1) is general, the scope of identification is limited by the available forecast data. Since the data consist primarily of inflation and output growth forecasts, I focus on two reduced-form shocks, which are labeled "supply" and "demand." These labels serve as convenient sign conventions and should be interpreted broadly, as they may capture a range of underlying structural disturbances.

However, agents may have their subjective models of the economy that differ from the true DGP. In particular, I assume that the agents have a misspecified model in terms of the loadings and long-run mean:

$$\mathbf{x}_t = \boldsymbol{\mu}_i + \mathbf{A}_i\left(\mathbf{x}_{t-1} - \boldsymbol{\mu}_i\right) + \mathbf{B}_i\boldsymbol{\epsilon}_t \tag{2}$$

This reflects the first non-information heterogeneity that agents have different perceived laws of motion of the economy that need not coincide with the true DGP (Marcet and Sargent, 1989; Bray and Savin, 1986; Andre et al., 2022; Crump, Eusepi, and Moench, 2024) and particularly relates to the misperception of persistence (Ryngaert, 2017; Angeletos, Huo, and K. A. Sastry, 2021). It is assumed that forecasters perceive two reduced form shocks, supply and demand. However, no restriction is placed on the perceived matrices $\mathbf{A}_i$ and $\mathbf{B}_i$, so forecasters may have heterogeneous and even unconventional views on how supply and demand shocks propagate (Andre et al., 2022; Hou and Wang, 2025). As discussed later in more detail, the sign restrictions used for empirical identification do not require $\mathbf{B}_i$ to follow the conventional supply and demand signs.

In addition, they can only observe noisy signals of $\mathbf{x}_t$. Assuming that only private signals are available, the signals are described by the following equation:

$$\mathbf{s}_{it} = \mathbf{x}_t + \mathbf{w}_{it} \tag{3}$$

In equation (3), the vector $\mathbf{s}_{it} = (s^x_{it})_{x\in\mathbf{x}}$ contains signals for macro aggregates. $\mathbf{w}_{it} = (w^x_{it})_{x\in\mathbf{x}}$ is the vector of noise specific to each target variable. Furthermore, it is also assumed that the noise for the state variables shares two common shocks, namely supply and demand noise shocks.

$$\mathbf{w}_{it} = \mathbf{\Sigma}_i \mathbf{u}_{it} \tag{4}$$

The supply and demand noise shocks, $\mathbf{u}_{it} = (u^s_{it}, u^d_{it})'$, are independent of each other, over time, across forecasters, and of the aggregate shocks, with a mean of zero and unit variances. The loadings on these noise shocks, $\mathbf{\Sigma}_i$, are assumed to follow signs that align with the supply-demand convention. For instance, the supply (demand) noise shock would affect the signal of growth and inflation in opposite (same) directions. Noise shocks are irrelevant for the actual DGP (1), meaning they do not impact aggregate variables directly, as opposed to aggregate shocks ($\boldsymbol{\epsilon}_t$). In other words, while the signals are variable-specific, they are correlated due to common noise components.

Incorporating common components of noise acknowledges the correlation in measurement errors across target variables. This is motivated by the idea of rational inattention (Sims, 2003) and the understanding that forecasters generate joint multivariate forecasts rather than separate univariate forecasts (Dovern, Fritsche, and Slacalek, 2012; Dovern, 2015; Andrade, Crump, et al., 2016; Herbst and Winkler, 2026; Crump, Eusepi, Moench, and Preston, 2023). Professional forecasters who must allocate limited resources efficiently to deliver accurate multivariate forecasts may measure these variables jointly, leading to correlated

measurement errors.

Moreover, the loadings ($\mathbf{\Sigma}_i$) are forecaster-specific, so the true precision of signals varies across forecasters. This reflects the second heterogeneity other than dispersed information (e.g. forecasting abilities). Furthermore, just as forecasters may perceive the propagation of aggregate shocks differently ($\mathbf{B}_i$ vs. $\mathbf{B}$), their perceived precision of signals (say, $\mathbf{\Sigma}_i^{\text{perceived}}$) could be different from the true precision ($\mathbf{\Sigma}_i$) (Broer and Kohlhas, 2022). In other words, the sign conventions are imposed on the true $\mathbf{B}$ and $\mathbf{\Sigma}_i$ and the sign restrictions used in the empirical section do not necessarily require the forecasters to be aware of them.

If the agents adhere to Bayesian principles and shocks are normally distributed, the optimal one-step ahead forecast is represented by the Kalman Filter:

$$\mathbb{F}_{it}[\mathbf{x}_{t+1}] = \boldsymbol{\mu}_i + \mathbf{A}_i \left\{ \mathbf{G}_i \left(\mathbf{s}_{it} - \boldsymbol{\mu}_i \right) + \left(\mathbf{I} - \mathbf{G}_i \right) \left(\mathbb{F}_{it-1}[\mathbf{x}_t] - \boldsymbol{\mu}_i \right) \right\} \tag{5}$$

In equation (5), $\mathbf{G}_i$ represents the forecaster-specific steady-state Kalman gain. The variation in Kalman gain across forecasters stems from the heterogeneous *perceived* precision of individual signals and different subjective models.[1] As will be explained in more detail in the next subsection, the sign restrictions in the empirical model will then require restrictions on $\mathbf{A}_i$ and $\mathbf{G}_i$, which govern how each forecaster updates expectations in response to signals.

2.2 A Factor Model of Professional Forecasts

Iterating over the recursive structure of the Kalman filter $\left(\mathbb{F}_{it}[\mathbf{x}_{t+1}]\right)$ in equation (5) reveals a factor structure of forecasts as shown in the following proposition. [2] The proofs of propositions are relegated to Appendix A.1.

Proposition 1. (Factor model of professional forecasts) *Suppose that the economy follows* (1) *and that forecaster i forms expectations using subjective models and belief-updating rules consistent with* (2), (3), (4), *and* (5). *Then the reported individual forecast implies the factor representation*

$$\mathbb{F}_{it}[\mathbf{x}_{t+1}] = \mathbf{b}_i + \sum_{k=0}^{\infty} \boldsymbol{\lambda}_{i,k} \boldsymbol{\epsilon}_{t-k} + \mathbf{v}_{it} \tag{6}$$

[1] Strategic incentives, such as herding or standing out, can also change the weight forecasters put on public relative to private information (Marinovic, Ottaviani, and Sorensen, 2013; Gemmi and Valchev, 2023). They would then be an additional source of heterogeneity in the effective Kalman gains, and hence in the loadings, as long as they are stable over time.

[2] The univariate version of this framework is presented in Juodis and Kučinskas (2023). Other forms of the factor structure of forecasts have also been documented and used in the literature: Herbst and Winkler (2026), Scanlan (2023).

where

$$
\begin{aligned}
\mathbf{b}_i &= \boldsymbol{\mu}_i + (\mathbf{I} - \boldsymbol{\rho}_i)^{-1} \mathbf{A}_i \mathbf{G}_i (\boldsymbol{\mu} - \boldsymbol{\mu}_i), \\
\boldsymbol{\lambda}_{i,k} &= \sum_{j=0}^{k} \boldsymbol{\rho}_i^j \mathbf{A}_i \mathbf{G}_i \mathbf{A}^{k-j} \mathbf{B}, \\
\mathbf{v}_{it} &= \boldsymbol{\rho}_i \mathbf{v}_{it-1} + \boldsymbol{\Phi}_i \mathbf{u}_{it}, \\
\boldsymbol{\rho}_i &= \Big(\mathbf{A}_i (\mathbf{I} - \mathbf{G}_i) \Big), \\
\boldsymbol{\Phi}_i &= \mathbf{A}_i \mathbf{G}_i \boldsymbol{\Sigma}_i.
\end{aligned}
$$

Equation (6) is essentially a generalized dynamic factor model in which the common components have an infinite moving average representation. The model captures three sources of disagreement. First, disagreement is generated through the forecaster-specific intercept for each variable ($\mathbf{b}_i$), which is referred to as the individual anchor. The anchor is the level to which the forecasts of forecaster i converge as the shocks decay. It does not necessarily coincide with the perceived long-run mean $\boldsymbol{\mu}_i$ because of the misspecification. Forecasters who perceive a higher (or lower) long-run mean have a higher (or lower) anchor and keep their forecasts persistently above (or below) the others.

Second, common, aggregate shocks transmit to disagreement through individual-specific loadings ($\boldsymbol{\lambda}_{i,k}$) that are functions of Kalman gains and the perceived DGP. Under FIRE, the Kalman gains would be an identity matrix and the agents would share the common knowledge of the actual DGP. This makes $\boldsymbol{\lambda}_{i,k}$ homogeneous across agents, preventing aggregate shocks from affecting forecaster disagreement.[3] The last source is the idiosyncratic noise shocks ($\mathbf{u}_{it}$), embedded in the residuals of VAR ($\mathbf{v}_{it}$). Under FIRE, there would be no information dispersion due to noise shocks, and hence no disagreement.

In equation (6), the loadings that govern the updating of expectations in response to contemporaneous common belief and noise shocks are

$$
\boldsymbol{\lambda}_{i,0} = \mathbf{A}_i \mathbf{G}_i \mathbf{B}, \quad \boldsymbol{\Phi}_i = \mathbf{A}_i \mathbf{G}_i \boldsymbol{\Sigma}_i.
$$

To clarify the assumptions that are required to impose the sign restrictions on the reduced-form loadings, $\boldsymbol{\lambda}_{i,0}$ and $\boldsymbol{\Phi}_i$, I first define the set of matrices that abide by the conventional sign restrictions. I then state more formally the assumption that $\mathbf{B}$ and $\boldsymbol{\Sigma}_i$ satisfy the conventional supply and demand sign restrictions.

[3] Under the same perceived law of motion, the disagreement would not be affected by aggregate shocks if signal precision is *homogeneous* as the Kalman gain would not be forecaster-specific (Coibion and Gorodnichenko, 2012).

Definition. Let $\mathcal{S}$ be the set of 2×2 matrices $\mathbf{S}$ with $\mathbf{S}_{11} > 0, \mathbf{S}_{12} > 0, \mathbf{S}_{21} < 0, \mathbf{S}_{22} > 0$.

The set $\mathcal{S}$ contains the set of matrices that implicitly assume the ordering of growth - inflation and supply- demand. It is assumed that $\mathbf{B}$ and $\mathbf{\Sigma}_i$ are elements of this set $\mathcal{S}$. Given this definition, the following proposition outlines the conditions for the sign restrictions on the reduced-form loadings.

Proposition 2. (Sign restriction) *Suppose there is a* 2×2 *matrix* $\mathbf{M}$*. Let* $\mathbf{S} \in \mathcal{S}$ *be given. Then* $\mathbf{MS} \in \mathcal{S}$ *if and only if*

(i) Expectation of a variable responds positively to its own signal:

$$\mathbf{M}_{11} > 0, \quad \mathbf{M}_{22} > 0$$

(ii) The cross-variable signal does not outweigh the own-variable signal:

$$\begin{aligned} -\frac{\mathbf{S}_{12}}{\mathbf{S}_{22}} < \frac{\mathbf{M}_{12}}{\mathbf{M}_{11}} < -\frac{\mathbf{S}_{11}}{\mathbf{S}_{21}}, \\ -\frac{\mathbf{S}_{22}}{\mathbf{S}_{12}} < \frac{\mathbf{M}_{21}}{\mathbf{M}_{22}} < -\frac{\mathbf{S}_{21}}{\mathbf{S}_{11}}. \end{aligned}$$

where $\mathbf{M}_{ij}$ *and* $\mathbf{S}_{ij}$ *denote the elements of row* i *and column* j*.*

The mapping matrix in the context of this paper's analysis is $\mathbf{M} \equiv \mathbf{A}_i\mathbf{G}_i$. The shocks first transmit to the signals through the true $\mathbf{B}$ or $\mathbf{\Sigma}_i$. The forecaster then updates her expectation based on the signals through $\mathbf{G}_i$ and iterates forward via $\mathbf{A}_i$. Intuitively, condition (i) requires that in this process, each variable's expectation should update positively in response to its own signal. A higher growth (inflation) signal should raise the growth (inflation) forecast.

Condition (ii) bounds the weight that forecasters puts on the cross-variable signal relative to its own signal in the expectation updating process. For example, $\frac{\mathbf{M}_{12}}{\mathbf{M}_{11}}$ captures the ratio of how much weight an individual's growth expectation puts on the inflation signal over the growth signal. The upper bound, $-\frac{\mathbf{S}_{11}}{\mathbf{S}_{21}}$, is the supply (noise or common) shock's loading on growth over inflation. If the bound is breached, that means the forecaster is relying more on the inflation signal than the growth signal when updating the growth expectation.

For example, suppose there is a forecaster who reads inflation news as positive growth news ($\mathbf{M}_{12} > 0$). After a positive supply shock that raises true growth and lowers inflation, the forecaster will receive two signals: one is a positive signal of growth and the other is a negative signal about inflation. For this forecaster, the former would indicate the positive updating of growth expectation, whereas the latter indicates the negative updating of growth expectation. Condition (ii) is setting the upper bound that the latter, cross-variable signal

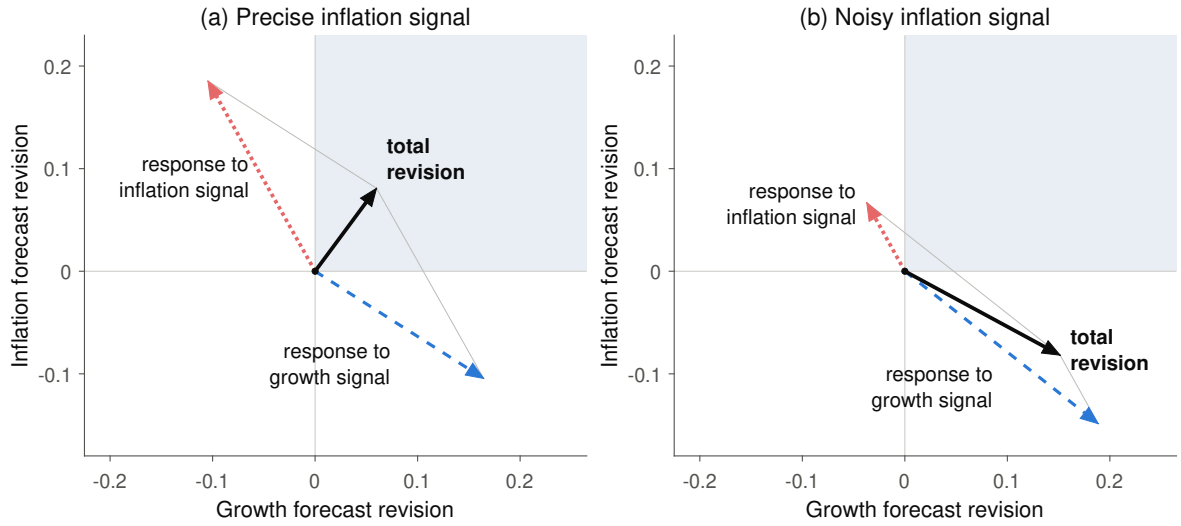

Figure 1: Illustration of Proposition 2.

Notes: The figure shows a numerical example where growth and inflation expectations revise after a positive demand shock. It assumes a forecaster who has stagflationary view regardless of the underlying shocks. The dotted, dashed, and solid arrows show the response to the inflation signal, the response to the growth signal, and the total revision. The shaded area marks the conventional response to a demand shock.

should exert a weaker influence than the former, own-variable signal, in the expectation formation process.

In contrast, the lower bound, $-\frac{\mathbf{S}_{12}}{\mathbf{S}_{22}}$, is the demand (noise or common) shock's loading on growth over inflation. Suppose there is a forecaster who reads inflation news as stagflationary, negative growth news ($\mathbf{M}_{12} < 0$). After a positive demand shock that raises true growth and inflation, the forecaster will again receive two positive signals about growth and inflation. For this forecaster, the former would indicate the positive updating of growth expectation, whereas the latter indicates the negative updating of growth expectation (due to the stagflationary view). Condition (ii) is setting the lower bound that the latter, cross-variable signal should not drive the direction of the growth expectation updating by outweighing the own-variable signal.

Figure 1 provides a visual illustration. Suppose that a positive demand shock hits the economy, but a forecaster has an unconventional view of shock transmission and always reads higher inflation as bad news for growth (stagflationary view). In both panels, the x and y axes represent the forecast revision of growth and inflation upon receiving the signals. The red dotted arrow shows how the forecaster revises growth and inflation expectations in response to the inflation signal alone. For this forecaster, a positive inflation signal induces an upward revision of inflation expectations, but a downward revision of growth expectations. The blue dashed arrow shows the revisions in response to the growth signal alone. The

forecaster revises the inflation expectation downward along with an upward revision of the growth expectation. The black solid arrow shows the total revision, which is what shows up in the data. The length of each arrow reflects the weight the forecaster places on each signal, which depends on how reliable the forecaster perceives the signal to be.

In panel (a), the own-variable signals, which respond to the demand shock in a conventional way, are strong enough that, even though the forecaster has a stagflationary view of how demand shocks propagate, the resulting revisions align with the conventional response to a demand shock. In contrast, in panel (b), the inflation signal is perceived to be less precise and unreliable. Therefore, the cross-variable signal for inflation, which is the growth signal, outweighs the weak own-variable signal. As a consequence, the forecaster relies more on the growth signal when updating the inflation expectation, and the unconventional view shows up in the data. Proposition 2 provides the conditions that rule out the case in panel (b).

As aforementioned, the sign restrictions are imposed on the true $\mathbf{B}$ and $\mathbf{\Sigma}_i$, not on the individual's perceived counterparts. The *perceived* matrices about the impact effect of the shock and signal precision only affect the loadings on the signal $\mathbf{G}_i$, and hence the mapping matrix $\mathbf{M}$. *The sign restrictions therefore only require discipline on how forecasters process the signals rather than how they perceive the propagation of shocks.* The supply and demand labels classify the shocks and hence the sources of disagreement by how they move the signals and the forecasts, not by how individual forecasters interpret them. The heterogeneous models of their transmission, whether they are conventional or not, are exactly what the heterogeneous loadings capture. For example, inflation disagreement could arise in response to a true, conventional supply shock because i) two forecasters may hold the conventional view but with different degrees, or ii) one holds the conventional view and the other holds an unconventional view. The empirical framework nests all these cases as long as the Proposition 2 holds.

Discussion Several points merit discussion. First, the factor model in equation (6) is derived from a DGP of a stationary VAR. However, recent literature, as summarized in (Crump, Eusepi, Moench, and Preston, 2023), highlights the importance of a trend-cycle model with shifting endpoints for explaining the joint term structures of forecasts. While the trend-cycle model also yields a factor representation similar to the one used in this paper, the choice of a stationary model is motivated by two key considerations. First, long-run forecasts of multiple variables for individual forecasters are difficult to obtain, limiting the feasibility of analysis. Second, this study focuses on 1-year-ahead forecasts, a relatively short horizon where the influence of shifting endpoints is likely to be less pronounced. A

joint analysis of multivariate and multi-horizon heterogeneous beliefs is left for future work.

Second, the baseline framework assumes the absence of a public signal. In practice, however, signals may also contain a common component that affects all forecasters. In this case, as noted by Juodis and Kučinskas (2023), the common factors would capture such common public noise shocks as well as the aggregate shocks. For this reason, I interpret the shocks identified from the factors as *common belief shocks* throughout the rest of the paper, and reserve the term *aggregate shocks* for the shocks actually hitting the economy. Likewise, their supply and demand labels should be understood as common shocks that shape belief updating, rather than literal structural shocks. The term noise shocks refers to the idiosyncratic noise shocks throughout the paper, since the common component of noise is absorbed by the common belief shocks.

Third, and relatedly, a more general interpretation of the individual fixed-effect term in equation (6) could also include the deviation of individual forecast from the optimal Bayesian forecast.[4] If there is some persistent forecaster heterogeneity, such as strategic interaction (Marinovic, Ottaviani, and Sorensen, 2013), heterogeneity in forecasting models (Giacomini, Skreta, and Turen, 2020) or asymmetric loss functions (Capistrán and Timmermann, 2009), the fixed effect would also linearly and additively capture it on top of the long-run anchor. Appendix D discusses how such individual biases can be interpreted through the framework of the latter two papers.[5] However, the estimates of the fixed effect in Section 3.3 suggest that it mainly reflects the long-run anchor rather than such deviations.

3 Empirical Framework

3.1 Data: Blue Chip Economic Indicators

The forecast data utilized in this study is the "Blue Chip Economic Indicators (BCEI)", a monthly survey that collects the opinions of around 50-60 experts on the U.S. economy. There are two reasons why BCEI is the most adequate dataset for the purpose of this paper. One is that, unlike other commonly used surveys, the monthly frequency of the survey allows for more observations per forecaster.[6] This is crucial because a higher number of

[4]The Bayesian principle refers to the optimal forecast in the sense of mean-squared error-minimization (i.e. the Kalman Filter). Deviation from this does not necessarily indicate the deviation from the Bayesian 'rationality'. For example, a rational Bayesian agent could have an asymmetric loss function and produce a forecast that differs from the mean-squared error-minimizing Bayesian forecast (Capistrán and Timmermann, 2009).

[5]Such biases can also take a more general form of deviation from the Bayesian principle. For a deeper discussion please see Taubinsky et al. (2024).

[6]See Giacomini, Skreta, and Turen (2020) and Crump, Eusepi, Moench, and Preston (2023) for a comparison of commonly used surveys of professional forecasters in research.

observations is advantageous for identifying idiosyncratic noise shocks. The other is that the participation of forecasters in BCEI is more consistent and stable, alleviating the issue of missing observations.

It is also important to distinguish BCEI from the Blue Chip Financial Forecasts (BCFF), which provides fixed-horizon forecasts of financial indicators. In addition to accessibility limitations, BCFF conducted surveys anonymously until the mid-1990s, making individual forecaster-level analysis infeasible beforehand. Given these constraints, BCEI is the more suitable dataset for this study.

However, BCEI collects fixed-event, calendar-year forecasts rather than fixed-horizon forecasts. To align with the empirical framework, fixed-horizon (1-year) forecasts are approximated by calculating a weighted average of the current and next calendar year forecasts, which is the convention used in the literature (Johnson, 2002; Dovern, Fritsche, and Slacalek, 2012; Siklos, 2013).[7]

In the baseline analysis, the sample period runs from 1984M7 to 2023M9.[8] To identify supply and demand shocks, forecasts of real output growth and inflation are used.[9] The baseline analysis excludes interest rate forecasts due to additional computational complexities in identifying supply and demand noise shocks, as detailed in Appendix E.1. However, as demonstrated in Appendix E.1, the core findings of the disagreement decomposition remain robust even when interest rate forecasts are included. Furthermore, forecasters with fewer than 60 observations are excluded to ensure a sufficient number of observations for individual optimization that obtains idiosyncratic noise shocks. Outliers are also addressed by removing forecasts that deviate more than five interquartile ranges from the median similar to Bordalo et al. (2020). Applying these criteria results in an unbalanced panel of 116 forecasters.[10]

Using this forecast sample, the consensus (cross-sectional mean) and disagreement (cross-sectional variance) are computed after approximating 1-year-ahead expectations. The results are presented in Figure 2, with shaded areas indicating NBER recessions. The blue solid lines from the cleaned sample, which excludes forecasters with limited coverage, closely track the black dashed lines from the original sample including all participants. This suggests that the cleaned sample of forecasters is sufficiently representative. In the upper-left panel, the

[7] If a participant at 1990M3 reported their current (1990) and next calendar year (1991) inflation rate as 2% and 6%, the 12-month ahead inflation forecast will be approximated as $\frac{3}{4} \cdot 2 + \frac{1}{4} \cdot 6 = 3\%$. Ganics, Rossi, and Sekhposyan (2024) show that this ad hoc weighting scheme performs as well as optimized weights most of the time.

[8] Prior to July 1984, the BCEI only published current-year forecasts, making it impossible to construct the fixed-horizon forecasts.

[9] In line with the convention in the literature, the GNP/GDP deflator inflation forecasts are used.

[10] Excluding participants with fewer than 60 observations removes roughly 12.4% of the total observations. The empirical results, however, remain robust when using lower thresholds for the minimum number of observations, as reported in Appendix E.6.

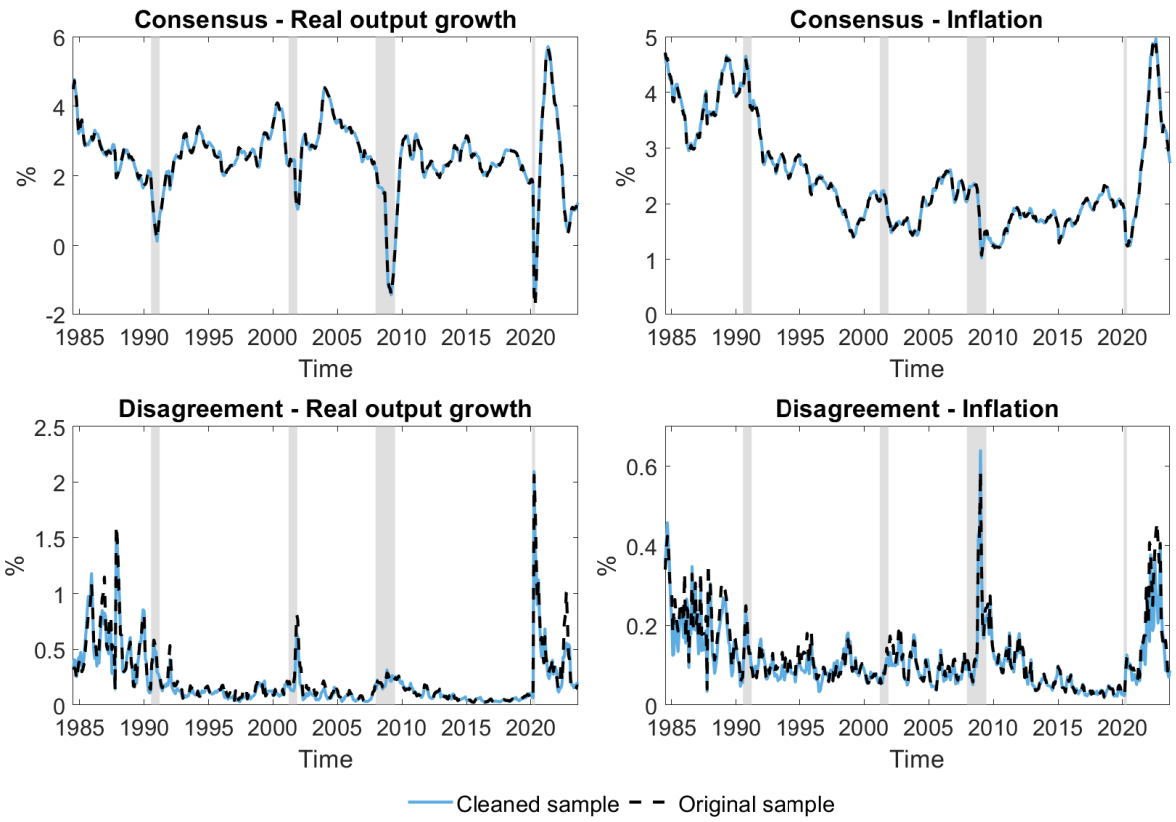

Figure 2: Consensus Forecast and Disagreement.

Notes: The figure illustrates the consensus and disagreement among forecasts after approximating the fixed-horizon (1-year ahead) forecasts from fixed-event forecasts (current and next calendar year). The top and bottom rows present the consensus and disagreement, computed as the cross-sectional mean and variance across forecasters; the left and right columns correspond to real output growth and inflation, respectively.

consensus forecast of real output growth is procyclical, falling sharply during each recession. In the upper-right panel, the consensus inflation forecast declines steadily through 2020 before rising sharply following the Covid-19 recession.

In the lower-left panel, the disagreement in real output growth forecasts is first characterized by heightened volatility in the 1980s and early 1990s. During this period, the cross-sectional dispersion exhibited significant fluctuations, ranging from around 0.5 to 1% squared. The peak of disagreement about real output growth was observed during the Covid-19 recession. Disagreement regarding inflation forecasts presented in the lower right panel also exhibited a similar pattern, although to a lesser extent. Although it is worth highlighting that disagreements regarding both variables tend to escalate during recessions, they are not strictly countercyclical. This observation serves as a distinctive characteristic of disagreement, as opposed to uncertainty, which negatively co-moves with the state of the economy as noted by Falck, Hoffmann, and Hürtgen (2021).

3.2 Empirical Model

The optimal h-step ahead forecast can be obtained by iterating the one-step ahead forecast over the DGP in equation (2). Building on this, the empirical factor model of h-step ahead forecast is postulated as follows.[11]

$$\mathbb{F}_{it}[\mathbf{x}_{t+h}] = \mathbf{b}_i + \boldsymbol{\lambda}_i \mathbf{f}_t + \mathbf{v}_{it}, \quad \mathbf{f}_t = \boldsymbol{\Gamma} \mathbf{f}_{t-1} + \boldsymbol{\epsilon}_t, \quad \mathbf{v}_{it} = \boldsymbol{\rho}_i \mathbf{v}_{it-1} + \boldsymbol{\Phi}_i \mathbf{u}_{it} \tag{7}$$

In equation (7), factors and residuals follow VAR processes.[12] For expositional clarity, the notations are written in VAR(1) form.[13] Each term captures one of the three sources of disagreement. The fixed effect ($\mathbf{b}_i = (b_i^g, b_i^\pi)'$) corresponds to the forecaster-by-variable specific anchor. The loadings ($\boldsymbol{\lambda}_i$) reflect the response of each forecaster's forecasts of the target variables ($\mathbf{x}_t = (g_t, \pi_t)'$) to common belief supply and demand shocks ($\boldsymbol{\epsilon}_t = (\epsilon_t^s, \epsilon_t^d)'$) that are embedded as the residuals of common factors ($\mathbf{f}_t = (f_t^s, f_t^d)'$).[14] Following Proposition 2, the loadings ($\boldsymbol{\lambda}_i$) are assumed to have signs that align with the conventional sign restrictions associated with supply and demand shocks. Idiosyncratic supply and demand noise shocks ($\mathbf{u}_{it} = (u_{it}^s, u_{it}^d)'$) are contained in the individual-specific VAR process of residuals ($\mathbf{v}_{it} = (v_{it}^g, v_{it}^\pi)'$). The loadings ($\boldsymbol{\Phi}_i$) are also assumed to have signs that adhere to the convention. Both common belief shocks and noise shocks are also assumed to have mean zero and unit variance.

The selection of two factors as the optimal number of factors is not a deliberate alignment with the supply-demand framework. As documented in Appendix B.1, two factors provide sufficient explanatory power for the real output growth and inflation forecast data. The marginal contributions from additional factors are small. A robustness check with an additional factor is provided in Appendix E.8. The factors are estimated via the iterative least squares (Bai, 2003; Bai, 2009), following the procedure outlined in Juodis and Kučinskas (2023).[15]

[11] The reduced form model essentially imposes $\boldsymbol{\lambda}_i(L)\boldsymbol{\epsilon}_t = \boldsymbol{\lambda}_i \mathbf{f}_t$ with $\mathbf{f}_t = \boldsymbol{\Gamma}\mathbf{f}_{t-1} + \boldsymbol{\epsilon}_t$ as in Herbst and Winkler (2026). However, the difference is that $\boldsymbol{\Gamma}$ may have non-zero, non-diagonal entries, whereas Herbst and Winkler (2026) assume that factors follow independent AR processes.

[12] h is dropped from the right-hand side since only one horizon (1-year) is being used.

[13] In the empirical application, the optimal lag length is chosen based on information criteria, and robustness checks with different lag lengths yield similar decomposition results.

[14] Although factors confound the lagged supply and demand shocks through the VAR structure, the supply and demand labels are retained as the residual of each factor corresponds to the current common belief supply and demand shocks.

[15] The estimation procedure is explained in Appendix B.2.

3.3 Identification of Common Belief Shocks

3.3.1 Identification Procedure

This section discusses the identification strategy of common belief supply and demand shocks ($\boldsymbol{\epsilon}_t = (\epsilon_t^s, \epsilon_t^d)'$). The estimated model would be

$$\mathbb{F}_{it}[\mathbf{x}_{t+h}] = \hat{\mathbf{b}}_i + \hat{\boldsymbol{\lambda}}_i \hat{\mathbf{f}}_t + \hat{\mathbf{v}}_{it} \tag{8}$$

The challenge with the factor model is that the estimated factors and loadings need not coincide with their latent counterparts. Put simply,

$$\hat{\boldsymbol{\lambda}}_i \hat{\mathbf{f}}_t = \boldsymbol{\lambda}_i \mathbf{f}_t \quad \text{but} \quad \hat{\boldsymbol{\lambda}}_i \neq \boldsymbol{\lambda}_i, \ \hat{\mathbf{f}}_t \neq \mathbf{f}_t$$

This also implies that running a VAR model on the estimated factors ($\hat{\mathbf{f}}_t$) would not recover the shocks of interest:

$$\hat{\mathbf{f}}_t = \hat{\boldsymbol{\Gamma}} \hat{\mathbf{f}}_{t-1} + \hat{\boldsymbol{\xi}}_t \quad \text{but} \quad \hat{\boldsymbol{\xi}}_t \neq \boldsymbol{\epsilon}_t$$

The residuals from the VAR model of estimated factors and the latent shocks differ in two aspects. One is that the supply and demand shocks are orthogonal and have unit variances. The other is that the associated loadings of the shocks satisfy the sign restrictions that are consistent with the conventional sign restrictions typically associated with supply and demand shocks. These are addressed through two sets of rotations.

In the first set, to achieve orthogonality and unit variance, the loadings and factors are rotated using the Cholesky decomposition of the estimated residuals ($\mathbb{VAR}(\hat{\boldsymbol{\xi}}_t) = \mathbf{Z}\mathbf{Z}'$). The rotated model would be

$$\mathbb{F}_{it}[\mathbf{x}_{t+h}] = \hat{\mathbf{b}}_i + (\hat{\boldsymbol{\lambda}}_i \mathbf{Z})(\mathbf{Z}^{-1}\hat{\mathbf{f}}_t) + \hat{\mathbf{v}}_{it} = \hat{\mathbf{b}}_i + \hat{\hat{\boldsymbol{\lambda}}}_i \hat{\hat{\mathbf{f}}}_t + \hat{\mathbf{v}}_{it} \tag{9}$$

The VAR model of the rotated factor ($\hat{\hat{\mathbf{f}}}_t$) would yield a set of residuals ($\hat{\hat{\boldsymbol{\xi}}}_t \equiv \mathbf{Z}^{-1}\hat{\boldsymbol{\xi}}_t$) that are scaled from the original residuals but uncorrelated and have unit variances ($\mathbb{VAR}(\mathbf{Z}^{-1}\hat{\boldsymbol{\xi}}_t) = \mathbf{I}$).

In the second set, the loadings and factors are rotated once more so that the rotated loading matrix ($\hat{\hat{\boldsymbol{\lambda}}}_i$) has signs that align with the conventional sign restrictions. This is achieved by partially relying on the identification method commonly used in sign-restriction VAR models (Uhlig, 2005).

Suppose there is an orthonormal matrix $\mathbf{Q}$ such that $\mathbf{Q}\mathbf{Q}' = \mathbf{I}$. The equation (9) is

rotated again using the orthonormal matrix $\mathbf{Q}$:

$$\mathbb{F}_{it}[\mathbf{x}_{t+h}] = \hat{\mathbf{b}}_i + (\hat{\tilde{\boldsymbol{\lambda}}}_i \mathbf{Q})(\mathbf{Q}' \hat{\tilde{\mathbf{f}}}_t) + \hat{\mathbf{v}}_{it} = \hat{\mathbf{b}}_i + \tilde{\boldsymbol{\lambda}}_i \tilde{\mathbf{f}}_t + \hat{\mathbf{v}}_{it} \tag{10}$$

Then, the goal is to draw $\mathbf{Q}$ in a manner that ensures that the sign restrictions are satisfied by $\tilde{\boldsymbol{\lambda}}_i$ for as many forecasters as possible [16]:

$$\tilde{\boldsymbol{\lambda}}_i \tilde{\mathbf{f}}_t = \begin{bmatrix} \tilde{\lambda}_i^{\text{gs}} > 0 & \tilde{\lambda}_i^{\text{gd}} > 0 \\ \tilde{\lambda}_i^{\pi\text{s}} < 0 & \tilde{\lambda}_i^{\pi\text{d}} > 0 \end{bmatrix} \begin{bmatrix} \tilde{f}_t^s \\ \tilde{f}_t^d \end{bmatrix}$$

For instance, $\lambda_i^{\pi\text{s}}$ and $\lambda_i^{\pi\text{d}}$, the second-row elements of $\tilde{\boldsymbol{\lambda}}_i$, are the loadings of the inflation forecast on the supply and demand factors that embed contemporaneous supply and demand shocks. To adhere to the convention, the loadings are constrained to be negative and positive, respectively.

To find the optimal rotation matrix, a two-step approach is adopted to determine the most relevant and unique matrix $\mathbf{Q}$. The approach involves maximizing the number of forecasters who meet the sign restrictions while minimizing the deviation of forecasters who fail to meet sign restrictions.

In the first step, the set $\boldsymbol{\Theta}$ is constructed, which contains matrices $\mathbf{Q}$ maximizing the number of forecasters meeting the sign restrictions. This step helps identify a subset of rotations that achieve the highest possible compliance with the sign restrictions.[17]

In the second step, if there are multiple matrices in $\boldsymbol{\Theta}$, the matrix $\mathbf{Q}^*$ with the minimum deviation from the desired sign restrictions is selected. This step ensures that the chosen $\mathbf{Q}^*$ most closely adheres to the intended sign restrictions. A formal representation of the criterion is

$$\begin{aligned} \mathbf{Q}^* = \underset{\mathbf{Q} \in \boldsymbol{\Theta}}{\text{argmin}} \sum_{i=1}^{N} \Big(& (\tilde{\lambda}_i^{gs})^2 \cdot \mathbb{1}(\tilde{\lambda}_i^{gs} < 0) + (\tilde{\lambda}_i^{gd})^2 \cdot \mathbb{1}(\tilde{\lambda}_i^{gd} < 0) \\ & + (\tilde{\lambda}_i^{\pi s})^2 \cdot \mathbb{1}(\tilde{\lambda}_i^{\pi s} > 0) + (\tilde{\lambda}_i^{\pi d})^2 \cdot \mathbb{1}(\tilde{\lambda}_i^{\pi d} < 0) \Big) \end{aligned} \tag{11}$$

where $\mathbb{1}(\cdot)$ is an indicator function that takes the value of 1 if sign restriction is not met and 0 otherwise. The matrix $\mathbf{Q}^*$ minimizes the objective function, which is defined as the sum of squared distances between zero and the loadings with incorrect signs of each forecaster.

[16] The orthonormality of $\mathbf{Q}$ preserves the variance of shocks ($\mathbb{VAR}(\mathbf{Q}' \hat{\tilde{\boldsymbol{\xi}}}_t) = \mathbf{I}$).

[17] In the baseline case, multiple matrices $\mathbf{Q}$ that satisfy the desired sign restrictions for 113 out of 116 forecasters had been identified. Matrices $\mathbf{Q}$ that satisfy the sign restrictions for more than 113 forecasters were not found. In this scenario, the set $\boldsymbol{\Theta}$ would contain these matrices $\mathbf{Q}$ that fulfill the sign restrictions for the 113 forecasters. Then, in the second step, $\mathbf{Q}^* \in \boldsymbol{\Theta}$ that solves criterion (11) is chosen.

Table 1: First stage estimation result: factor loadings and anchors

	$\hat{b}_i^g$	$\tilde{\lambda}_i^{gs}$	$\tilde{\lambda}_i^{gd}$	$\hat{b}_i^\pi$	$\tilde{\lambda}_i^{\pi s}$	$\tilde{\lambda}_i^{\pi d}$
P95	2.95	0.14	0.26	2.80	-0.03	0.10
P75	2.53	0.12	0.22	2.58	-0.06	0.07
P50	2.40	0.11	0.19	2.49	-0.07	0.05
P25	2.30	0.09	0.18	2.38	-0.08	0.04
P05	2.03	0.06	0.15	2.16	-0.10	0.02
IQR	0.24	0.03	0.04	0.20	0.02	0.03

Notes: This table presents the summary statistics of the estimated individual anchors ($\hat{\mathbf{b}}_i$) and loadings ($\tilde{\boldsymbol{\lambda}}_i$) on the common factors in equation (10). Specifically, $\hat{b}_i^{\mathrm{g}}$ and $\hat{b}_i^{\pi}$ represent the individual anchors for real output growth and inflation forecasts, respectively. $\tilde{\lambda}_i^{\mathrm{gs}}$ and $\tilde{\lambda}_i^{\pi\mathrm{s}}$ denote the individual-specific loadings on supply shocks to real output growth and inflation forecasts, whereas $\tilde{\lambda}_i^{\mathrm{gd}}$ and $\tilde{\lambda}_i^{\pi\mathrm{d}}$ indicate individual-specific loadings on demand shocks to real output growth and inflation forecasts. Each row shows the 95th, 75th, median, 25th, and 5th percentile values across 116 forecasters.

$\mathbf{Q}^*$ is then used to obtain the final-rotated factors ($\tilde{\mathbf{f}}_t$) and loadings ($\tilde{\boldsymbol{\lambda}}_i$) and the common belief shocks can be recovered by running the VAR model on factors.[18]

3.3.2 Identification Result

Table 1 provides an overview of the estimation result after the final rotation. Each row presents the percentile values of the estimated parameters across forecasters, offering insights into the distribution of the estimated individual anchors ($\hat{\mathbf{b}}_i$) and loadings ($\tilde{\boldsymbol{\lambda}}_i$) on the common factors in equation (10). The last row shows the interquartile range of these parameters.

More specifically, $\hat{b}_i^{\mathrm{g}}$ and $\hat{b}_i^{\pi}$ represent the individual anchors for real output growth and inflation forecasts, respectively. The estimates of the anchors for the two variables are similar in terms of both level and dispersion. The relatively large estimates of around 2–3% suggest that the anchors primarily reflect persistent differences in the perceived long-run levels across forecasters, rather than deviations from the optimal Bayesian forecast.

$\tilde{\lambda}_i^{\mathrm{gs}}$ and $\tilde{\lambda}_i^{\pi\mathrm{s}}$ denote the individual-specific loadings on supply shocks for real output growth and inflation forecasts, respectively. Similarly, $\tilde{\lambda}_i^{\mathrm{gd}}$ and $\tilde{\lambda}_i^{\pi\mathrm{d}}$ indicate individual-specific loadings on demand shocks. Each percentile value suggests that the loadings of growth forecasts are larger in magnitude than those of inflation forecasts. For example, the median values of the loadings of growth forecasts are 0.11 and 0.19, whereas they are -0.07 and 0.05 for inflation forecasts. This means one unit of common belief shock shifts the perception of growth more than inflation. Also, the loadings of growth forecasts are more responsive to

[18] In the baseline case, two lags are used in the VAR model as the information criteria points to two lags as optimal. However, the empirical results are robust to different lag lengths.

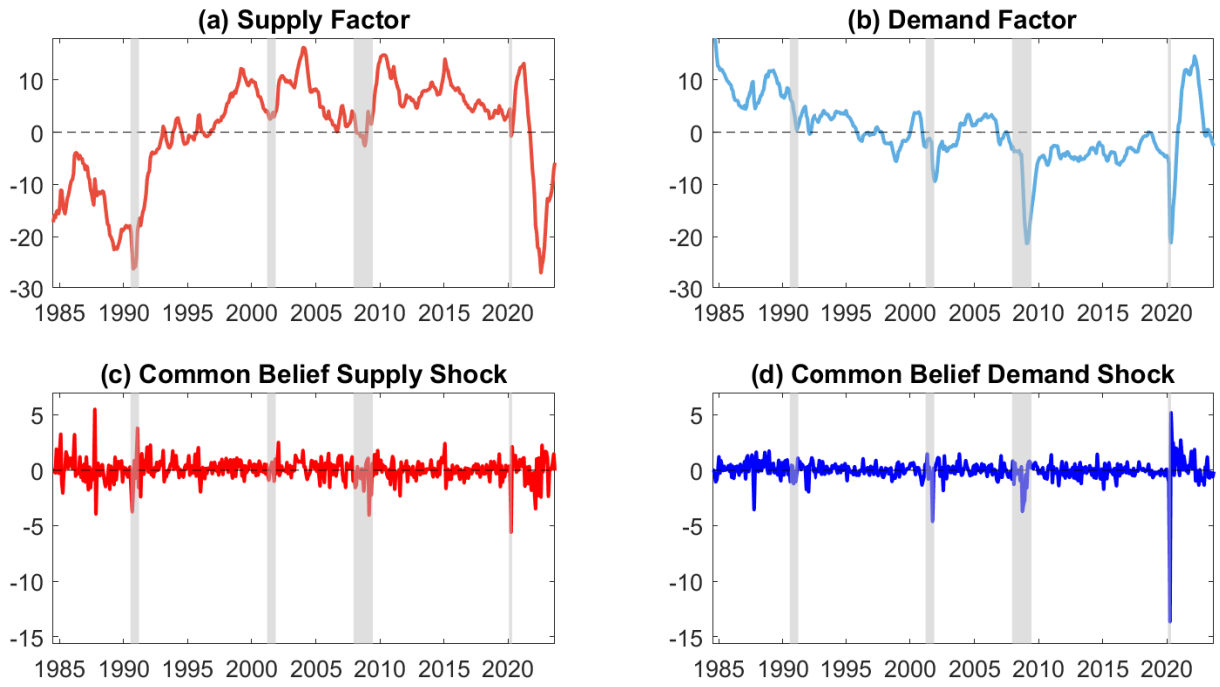

Figure 3: Supply and Demand Factors and Shocks.

Notes: The figure displays estimated supply and demand factors $\tilde{\mathbf{f}}_t = (\tilde{f}_t^s, \tilde{f}_t^d)'$ and common belief shocks $(\boldsymbol{\epsilon}_t = (\epsilon_t^s, \epsilon_t^d)')$ over the sample period. The shaded areas indicate NBER recessions.

demand shocks than supply shocks.

Figure 3 displays the estimated factors (upper panel) and common belief shocks (lower panel). Both factors are highly serially correlated, whereas common belief supply and demand shocks are not serially correlated and are largely negative during the four recessions in the sample. Negative supply shocks are more pronounced during the Gulf War recession in the early 1990s, whereas negative demand shocks are more notable in other recessions. Appendix E.4 documents that the identified common belief shocks also yield impulse responses of macroeconomic variables that align with the conventional intuition.

A common disturbance that moves beliefs as if it were a supply or demand shock need not correspond one-for-one to an actual aggregate shock hitting the economy. To examine this, the aggregate supply and demand shocks are identified from the realized data of real output growth and inflation, using the higher-order moment strategy which gives point-identification. The details of the estimation are available in Appendix C. Figure 4 compares the aggregate shocks based on the realized data with the common belief shocks. The common belief shocks are summed over the three months within a quarter to compare with the aggregate shocks that are identified at the quarterly frequency. Both types of shocks show

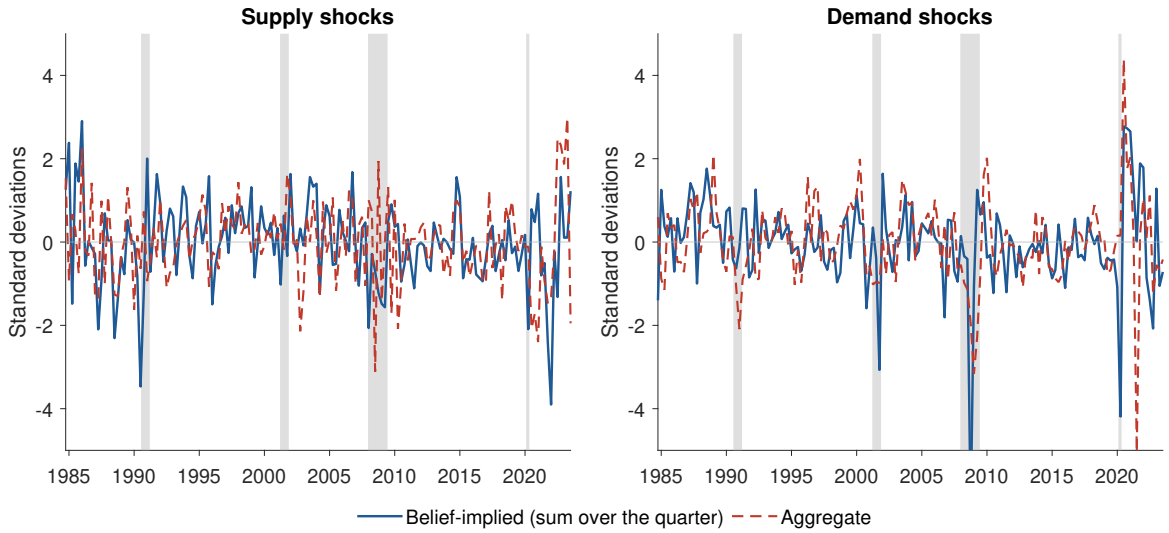

Figure 4: Supply and Demand shocks: Belief-implied vs. Aggregate.

Notes: The figure displays the belief-implied shocks, summed over the three months of each quarter, and the aggregate shocks. The shaded areas indicate NBER recessions.

similar spikes and signs during major economic events.[19]

Table 2 reports the correlations between the two types of shocks. Panel A shows the correlation between aggregate shocks and the common belief shocks summed over different months. For example, Months 1–3 indicates the summation over months within the same quarter, whereas Months 3–5 means summation over the last month of a quarter and the two months of the subsequent quarter. Panel B shows the correlation with each month's common belief shock estimate within a quarter.

Within a quarter, the correlation is 0.34 for demand and 0.17 for supply. The two shocks are therefore related but not identical, which is consistent with the common belief shocks capturing common signals as well as the aggregate shocks. Also, as Panel B shows, the correlation for demand is already sizable in the first two months of the quarter (0.17 and 0.26), before any data on the quarter are released. In contrast, the correlation for supply peaks later with Months 3–5 (0.51), and is higher than over the contemporaneous quarter (0.17). This may reflect either a relatively longer lag for supply shocks to reach the forecasters' perceptions, or much noisier supply-related news.

[19]The estimation dummies out 2020Q1, 2020Q2, and 2021Q2 associated with outlier observations of real GDP growth during Covid and base effects in the following year. As a consequence, the aggregate shocks for the three periods are mechanically set to zero.

Table 2: Correlation between belief-implied and aggregate shocks

	Supply	Demand
Panel A: Common belief shocks summed over		
Months 1–3 (the same quarter)	0.17	0.34
Months 2–4	0.36	0.31
Months 3–5	0.51	0.32
Panel B: Common belief shocks within a quarter		
Month 1	−0.06	0.17
Month 2	0.06	0.26
Month 3	0.28	0.27

Notes: Correlation between the monthly belief-implied shocks, summed over the months shown, and the quarterly aggregate shocks based on realized data. Months 1, 2, and 3 refer to the first, second and third month of the quarter. Months 4 and 5 belong to the subsequent quarter. The sample is 1984:Q4–2023:Q2 (152 quarters), excluding 2020:Q1, 2020:Q2 and 2021:Q2.

3.4 Identification of Idiosyncratic Noise Shocks

3.4.1 Identification Procedure

The focus now shifts to the identification of idiosyncratic noise shocks. Firstly, obtain the residuals from the estimated factor model (10): $\hat{\mathbf{v}}_{it} = \mathbb{F}_{it}[\mathbf{x}_{t+h}] - \hat{\mathbf{b}}_i - \tilde{\boldsymbol{\lambda}}_i \tilde{\mathbf{f}}_t$. Second, running VAR on the residual vectors ($\hat{\mathbf{v}}_{it} = (v_{it}^g, v_{it}^\pi)'$) separately for each forecaster yields errors that are a function of supply and demand noise:[20]

$$\hat{\mathbf{v}}_{it} = \hat{\boldsymbol{\rho}}_i \hat{\mathbf{v}}_{it-1} + \hat{\mathbf{e}}_{it}, \quad \hat{\mathbf{e}}_{it} = \boldsymbol{\Phi}_i \mathbf{u}_{it} \quad \Leftrightarrow \quad \begin{cases} \hat{e}_{it}^g &= \phi_i^{gs} u_{it}^s + \phi_i^{gd} u_{it}^d \\ \hat{e}_{it}^\pi &= -\phi_i^{\pi s} u_{it}^s + \phi_i^{\pi d} u_{it}^d \end{cases} \tag{12}$$

$\mathbf{u}_{it} = (u_{it}^s, u_{it}^d)'$ is a vector of noise shocks. $\boldsymbol{\Phi}_i = (\phi_i^{\text{gs}}, \phi_i^{\pi\text{s}}, \phi_i^{\text{gd}}, \phi_i^{\pi\text{d}})'$ represents the individual-specific loadings on supply and demand noise shocks for real output growth and inflation forecasts. The loadings are assumed to be positive. The noise shocks are assumed to be mutually independent with mean zero and unit variance.

Third, the loadings can then be estimated by relying on the higher-order moment identification strategy.[21] In particular, the estimation closely follows the strategy proposed in Bekaert, Engstrom, and Ermolov (2021) that identifies supply and demand shocks by ap-

[20] VAR lag length is chosen individually based on BIC. However, the results are robust to different information criteria and even when the same number of lags are imposed on forecasters.

[21] Higher-order moments are favored over conventional sign restrictions for identification because they offer precise point identification, while the latter yields set identification (Uhlig, 2005). For the latter, the choice within the identified set greatly influences disagreement decomposition outcomes, as detailed in the Appendix E.2.

plying a classical minimum distance (CMD) approach to the forecast data.[22]

To proceed further, the CMD estimators are obtained by minimizing the objective function for each forecaster:

$$\hat{\boldsymbol{\theta}}_i = \underset{\boldsymbol{\theta}_i}{\operatorname{argmin}} \left\{ \left(\hat{\mathbf{m}}_i - \mathbf{m}_i(\boldsymbol{\theta}_i) \right)' \widehat{\mathbf{W}}_i \left(\hat{\mathbf{m}}_i - \mathbf{m}_i(\boldsymbol{\theta}_i) \right) \right\} \tag{13}$$

where $\widehat{\mathbf{W}}_i$ is the optimal weight matrix which in the baseline case is set to identity matrix due to small sample error. $\hat{\mathbf{m}}_i$ is the vector of sample moments from the data and $\mathbf{m}_i(\boldsymbol{\theta}_i)$ is the vector of corresponding moments from the linear model (12) that are functions of parameters to be estimated ($\boldsymbol{\theta}_i$).

The parameter $\boldsymbol{\theta}_i$ includes the four loadings on noise shocks ($\boldsymbol{\Phi}_i$), which means identification requires at least four moment conditions. However, there are only three moments available up to the second order: two variances and one covariance of $\hat{e}^g_{it}$ and $\hat{e}^\pi_{it}$. To address this identification challenge, information from higher-order moments in the data is leveraged.

Following the approach of Bekaert, Engstrom, and Ermolov (2021), fourth-order moments are incorporated into the estimation. Specifically, in addition to the three second-order moments, two measures of kurtosis and three measures of co-kurtosis are added. The motivation for the decision to use fourth-order moments instead of third-order moments (such as skewness and co-skewness) is twofold. One is that the fourth-order moments in the data are more statistically significant than third-order moments as in Bekaert, Engstrom, and Ermolov (2021). The other is that since individual forecast series are short, using too many moment conditions in this setup could lead to small sample bias (Altonji and Segal, 1996).

In summary, the CMD estimation (13) is based on eight moment conditions. These moment conditions include two standard deviations of $\hat{e}^g_{it}$ and $\hat{e}^\pi_{it}$, one correlation between $\hat{e}^g_{it}$ and $\hat{e}^\pi_{it}$, two kurtosis of $\hat{e}^g_{it}$ and $\hat{e}^\pi_{it}$ and three co-kurtosis of $\hat{e}^g_{it}$ and $\hat{e}^\pi_{it}$. These sample moments are matched with the corresponding moment conditions that are functions of parameters of the empirical model (12). The analytical expressions for $\mathbf{m}_i(\boldsymbol{\theta})$ are presented in Appendix B.4. In addition to the four loadings, the moment conditions derived from the linear model (12) require estimating kurtosis of supply and demand noise shocks (κ^s_i, κ^d_i). Therefore, the estimation includes a total of six parameters ($\boldsymbol{\theta}_i = [\phi^{gs}_i, \phi^{gd}_i, \phi^{\pi s}_i, \phi^{\pi d}_i, \kappa^s_i, \kappa^d_i]$) with eight moment conditions available. For each forecaster, the parameters are estimated using an optimal subset of moment conditions that is selected based on the moment selection criterion

[22]The literature indicates that for applying higher-order moments, shocks must be non-Gaussian (Montiel Olea, Plagborg-Møller, and Qian, 2022). However, as Juodis and Kučinskas (2023) notes, the linear factor structure in forecasts applies broadly, not just to this model, and does not depend on Gaussianity. Nonetheless, the noisy information model remains a valuable reference for the semi-structural interpretation of the factor model.

Table 3: Second stage estimation result: individual noise shock parameters

A. Fraction of forecasters by the number of moment conditions

	6	7	8
Fraction	0.27	0.73	0.00

B. Fraction of forecasters using each moment condition

	$\mathbb{E}[(e^{\pi}_{it})^2]$	$\mathbb{E}[(e^{g}_{it})^2]$	$\mathbb{E}[e^{g}_{it}e^{\pi}_{it}]$		
Fraction	1.00	1.00	0.97		
	$\mathbb{E}[(e^{\pi}_{it})^4]$	$\mathbb{E}[(e^{g}_{it})^4]$	$\mathbb{E}[(e^{g}_{it})(e^{\pi}_{it})^3]$	$\mathbb{E}[(e^{g}_{it})^3(e^{\pi}_{it})]$	$\mathbb{E}[(e^{g}_{it})^2(e^{\pi}_{it})^2]$
Fraction	0.91	0.96	0.89	0.78	0.24

C. Cross-sectional distribution of parameters

	$\hat{\phi}^{gs}_i$	$\hat{\phi}^{gd}_i$	$\hat{\phi}^{\pi s}_i$	$\hat{\phi}^{\pi d}_i$	$\hat{\kappa}^{s}_i$	$\hat{\kappa}^{d}_i$
P95	0.26	0.30	0.22	0.24	19.50	31.22
P75	0.18	0.19	0.17	0.15	9.64	11.47
P50	0.11	0.13	0.11	0.10	6.44	6.94
P25	0.03	0.04	0.03	0.02	5.05	4.78
P05	0.00	0.00	0.00	0.01	3.03	1.68
IQR	0.15	0.15	0.14	0.13	4.59	6.70

Notes: This table presents the summary statistics of the Classical Minimum Distance (CMD) estimation result of (13). Panel A reports the distribution of forecasters based on the number of moment conditions selected using the moment selection criterion of Andrews and Lu (2001). Panel B presents the fraction of forecasters whose optimal set of moment conditions includes each specific moment. $\hat{\phi}^{\text{gs}}_i$ and $\hat{\phi}^{\pi\text{s}}_i$ denote the individual-specific loadings on supply noise shocks to real output growth and inflation forecasts, whereas $\hat{\phi}^{\text{gd}}_i$ and $\hat{\phi}^{\pi\text{d}}_i$ indicate individual-specific loadings on demand noise shocks to real output growth and inflation forecasts. $\hat{\kappa}^{s}_i$ and $\hat{\kappa}^{d}_i$ represent the estimated kurtosis of individual supply and demand noise shocks. All loadings are reported as the positive parameters of equation (12); $\phi^{\pi s}_i$ enters the inflation equation with a negative sign by the supply–demand convention. Each row shows the 95th, 75th, median, 25th, and 5th percentile values across 116 forecasters.

of Andrews and Lu (2001).[23] After the parameters are estimated, the individual supply and demand noise shocks can be simply backed out for each forecaster by applying $\mathbf{u}_{it} = \hat{\mathbf{\Phi}}_i^{-1}\hat{\mathbf{e}}_{it}$.

3.4.2 Identification Result

Table 3 summarizes the estimation results. Panel A reports the distribution of forecasters based on the number of moment conditions selected using the moment selection criterion of Andrews and Lu (2001). Around 73% of forecasters are over-identified, selecting seven

[23]The detailed procedure of estimation is outlined in Appendix B.3.

out of eight available moment conditions to estimate six parameters. Notably, all of these forecasters fail to reject the null hypothesis in the overidentifying restrictions test, supporting the validity of the selected moment conditions.

Panel B presents the fraction of forecasters whose optimal moment set includes each specific moment condition.[24] The first row reports the inclusion rates for second-order moments (variances and covariance of inflation and growth errors), while the second row shows the inclusion rates for fourth-order moments (kurtosis and co-kurtosis). Nearly all forecasters incorporate second moments, highlighting their informativeness. Among fourth-order moments, independent kurtosis measures are used by over 90% of forecasters, whereas co-kurtosis measures are selected less frequently.

Each row of Panel C presents the percentile value of the estimated parameters across forecasters. It is observed that the median values (0.10 to 0.13) and dispersions (0.13 to 0.15) of the loadings are quite similar. This contrasts with Table 1 where inflation forecasts were less responsive to common belief shocks than growth forecasts. Moreover, as shown in Section 4.1, survey expectations exhibit short-lived impulse responses to noise shocks, whereas responses to common belief shocks are more persistent.

The last two columns of Table 3 provide insights into the distribution of noise shocks across individuals. The kurtosis of demand noise shocks exhibits greater dispersion than that of supply noise shocks, indicating that demand noise is more heterogeneous across forecasters.

Figure 5 depicts a time series pattern of estimated idiosyncratic supply (u_{it}^s) and demand (u_{it}^d) noise shocks. In panels (a) and (b), the blue, black, and red lines represent the 95th, 50th (median), and 5th percentile values of the estimated supply and demand noise shocks, respectively, at each cross-section. These figures suggest that the central tendency of the cross-sectional distribution of supply and demand noise shocks is consistently positioned around zero. However, the gap between 95th and 5th percentile values fluctuates countercyclically. Panels (c) and (d), which present the cross-sectional dispersion (IQR) of supply and demand noise shocks also attest to this point. The dispersion in noise shocks rises markedly in the four recessions in the sample.

[24] In the estimation, the moment conditions used for kurtosis are *excess* kurtosis, as detailed in Appendix B.4. For brevity, they are not explicitly expressed in excess terms here.

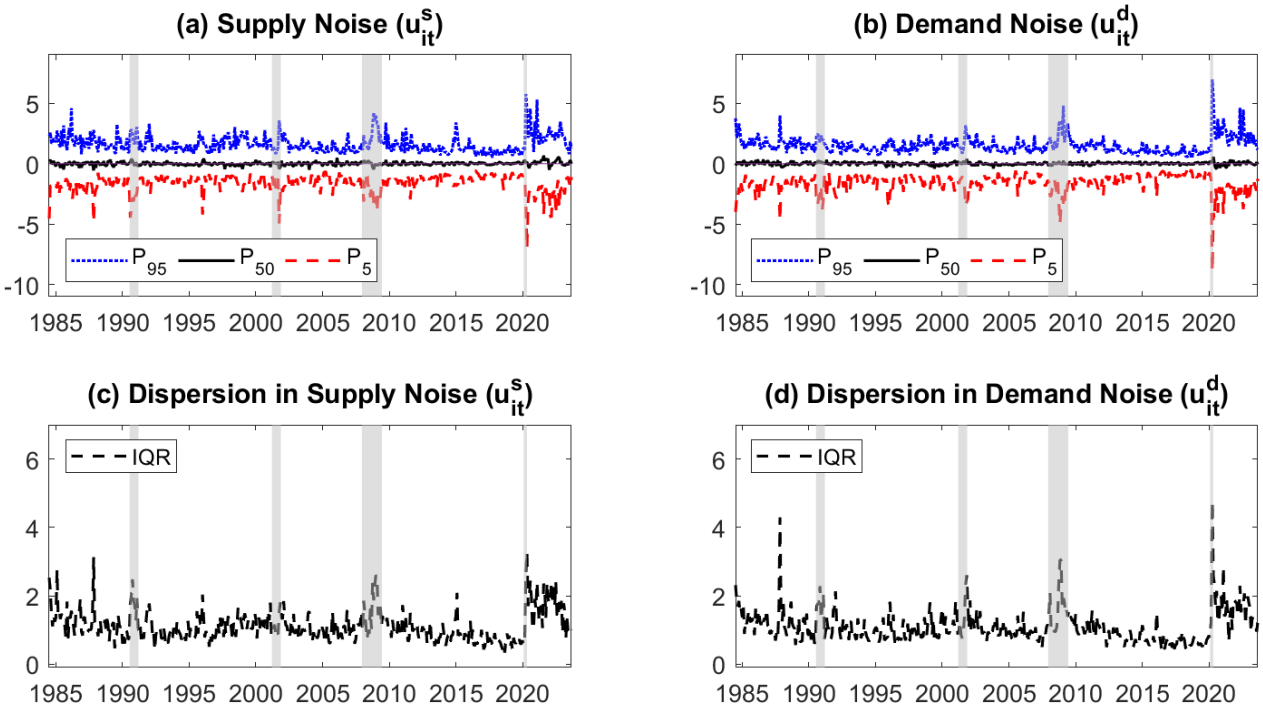

Figure 5: Idiosyncratic Supply and Demand Noise Shocks.

Notes: Panels (a) and (b) display the estimated supply (u_{it}^s) and demand (u_{it}^d) noise shocks over the sample period 1984M7-2023M9. The blue, black, and red lines represent 95th, 50th, and 5th percentile values, respectively. Panels (c) and (d) present the cross-sectional dispersion of supply and demand noise, measured by the interquartile range across forecasters that are active at each time period. The shaded areas indicate NBER recessions.

4 Empirical Results

4.1 Dynamic Effects of Common Belief versus Idiosyncratic Noise Shocks

Before turning to the decomposition, this section examines the dynamic effects of the identified shocks on macroeconomic expectations, which serves two purposes. First, it validates the identification: the responses should align with the supply and demand convention, not only with the growth and inflation forecasts that are used in the identification, but also with the interest rate forecast, which is not used in the identification. Second, it characterizes the behavioral distinction between the two types of shocks, common belief versus idiosyncratic noise. The impulse response functions (IRFs) are estimated using local projections following Jordà (2005).

Since common belief and idiosyncratic noise shocks enter at different levels of aggregation,

two specifications are estimated. For the IRFs to the common belief shocks, the specification is

$$y^f_{i,t+h} = \alpha_{i,h} + \beta_{s,h}\hat{\epsilon}^s_t + \beta_{d,h}\hat{\epsilon}^d_t + \mathbf{\Gamma}'_h\mathbf{X}_{it} + e_{i,t+h} \tag{14}$$

where $y^f_{i,t+h}$ denotes forecaster i's forecast of real output growth, inflation, or the interest rate h months ahead, $\alpha_{i,h}$ is a forecaster fixed effect, and $\mathbf{X}_{it}$ contains six lags of the dependent forecast variable and of the shocks. Time fixed effects cannot be included as they would absorb the common belief shocks themselves.

For the IRFs to the idiosyncratic noise shocks that are forecaster-specific, the specification adds time fixed effects ($\delta_{t,h}$):

$$y^f_{i,t+h} = \alpha_{i,h} + \delta_{t,h} + \beta_{s,h}\hat{u}^s_{it} + \beta_{d,h}\hat{u}^d_{it} + \mathbf{\Gamma}'_h\mathbf{X}_{it} + e_{i,t+h} \tag{15}$$

The time fixed effects absorb all variation common to forecasters, so that the coefficients are identified from the variation in the idiosyncratic shocks.

Figure 6 presents the estimated impulse responses. Each row corresponds to one of the forecast variables used as the dependent variable. The left column shows responses to common belief shocks, while the right column presents responses to noise shocks. Red solid lines indicate responses to supply-type shocks, and blue dashed lines represent responses to demand-type shocks. The shaded areas denote 90% confidence bands, computed using the Driscoll and Kraay (1998) standard errors.

The responses are broadly consistent with conventional economic theory. Real output growth forecasts respond positively to both supply and demand shocks, whereas inflation forecasts react with opposite signs. Moreover, interest rate forecasts respond positively to demand shocks but exhibit no significant response to supply shocks, suggesting a monetary policy tradeoff associated with supply shocks. The result implies that the forecasters' perceptions are consistent with a Taylor rule-type policy reaction function (Bauer, Pflueger, and Sunderam, 2024; Kim, 2026), and the effects of the supply and demand shocks on interest rate expectations are consistent with Herbst and Winkler (2026).[25]

A key distinction between common belief shocks and idiosyncratic noise shocks is the persistence of their effects. Common belief shocks generate persistent revisions in macroeconomic expectations, whereas the effects of idiosyncratic noise shocks dissipate rapidly and become statistically insignificant within a few months. This difference has important implications for the persistence of disagreement. To the extent that disagreement influences

[25] Appendix E.4 complements this evidence with impulse responses of realized macroeconomic variables to the identified common belief shocks, which also align with conventional intuition.

macroeconomic dynamics, disagreement generated by idiosyncratic noise is likely to be transitory, while disagreement arising from common belief shocks is likely to persist considerably longer, leaving a more durable imprint on aggregate expectations and macroeconomic outcomes.

4.2 Sources of Disagreement

4.2.1 Decomposition Method

After the rotations and identifications, for a target variable $x \in \{g, \pi\}$, the scalar representation of equation (10) is

$$\mathbb{F}_{it}[x_{t+h}] = \hat{b}_i^x + \underbrace{\tilde{\lambda}_i^{xs}\tilde{f}_t^s + \tilde{\lambda}_i^{xd}\tilde{f}_t^d}_{\tilde{\boldsymbol{\lambda}}_i{}'\tilde{\mathbf{f}}_t} + \underbrace{\hat{v}_{it}^x}_{\hat{\mathbf{v}}_{it}} \tag{16}$$

Iterating on the factors ($\tilde{\mathbf{f}}_t$) and the residual term ($\hat{\mathbf{v}}_{it}$) using their respective VAR models reformulates equation (16) as

$$\mathbb{F}_{it}[x_{t+h}] = b_i^x + \underbrace{\sum_{k=0}^{t}\left(\gamma_{i,k}^{xs}\epsilon_{t-k}^s + \gamma_{i,k}^{xd}\epsilon_{t-k}^d\right)}_{\text{Common belief shocks}} + \underbrace{\sum_{\ell=0}^{L_i}\left(\theta_{i,\ell}^{xs}u_{it-\ell}^s + \theta_{i,\ell}^{xd}u_{it-\ell}^d\right)}_{\text{Noise shocks}} \tag{17}$$

for some loadings ($\gamma_{i,k}^{xs}$, $\gamma_{i,k}^{xd}$, $\theta_{i,\ell}^{xs}$, $\theta_{i,\ell}^{xd}$) on lagged common belief and noise shocks. L_i denotes the number of lags, which depends on the participation status of each forecaster. Equation (17) illustrates clearly how individual forecasts are influenced by the current and lagged common belief and noise shocks. Additionally, the disagreement among forecasters, measured by the cross-sectional variance conditional on each time t, can be decomposed as follows:[26]

$$\begin{aligned}
\mathbb{VAR}_t\left[\mathbb{F}_{it}[x_{t+h}]\right] &= \underbrace{\mathbb{COV}_t\left[\mathbb{F}_{it}[x_{t+h}], \hat{b}_i^x\right]}_{\text{(a) Anchor}} \\
&+ \underbrace{\mathbb{COV}_t\left[\mathbb{F}_{it}[x_{t+h}], \sum_{k=0}^{t}\gamma_{i,k}^{xs}\epsilon_{t-k}^s\right]}_{\text{(b) Common Supply (C.S.)}} + \underbrace{\mathbb{COV}_t\left[\mathbb{F}_{it}[x_{t+h}], \sum_{k=0}^{t}\gamma_{i,k}^{xd}\epsilon_{t-k}^d\right]}_{\text{(c) Common Demand (C.D.)}} \\
&+ \underbrace{\mathbb{COV}_t\left[\mathbb{F}_{it}[x_{t+h}], \sum_{\ell=0}^{L_i}\theta_{i,\ell}^{xs}u_{it-\ell}^s\right]}_{\text{(d) Supply Noise (S.N.)}} + \underbrace{\mathbb{COV}_t\left[\mathbb{F}_{it}[x_{t+h}], \sum_{\ell=0}^{L_i}\theta_{i,\ell}^{xd}u_{it-\ell}^d\right]}_{\text{(e) Demand Noise (D.N.)}}
\end{aligned} \tag{18}$$

[26] The decomposition (18) utilizes the following property of covariance: For random variables X, Y, and Z, if $Z = X + Y$, then $\mathbb{VAR}(Z) = \mathbb{COV}(Z, Z) = \mathbb{COV}(Z, X + Y) = \mathbb{COV}(Z, X) + \mathbb{COV}(Z, Y)$.

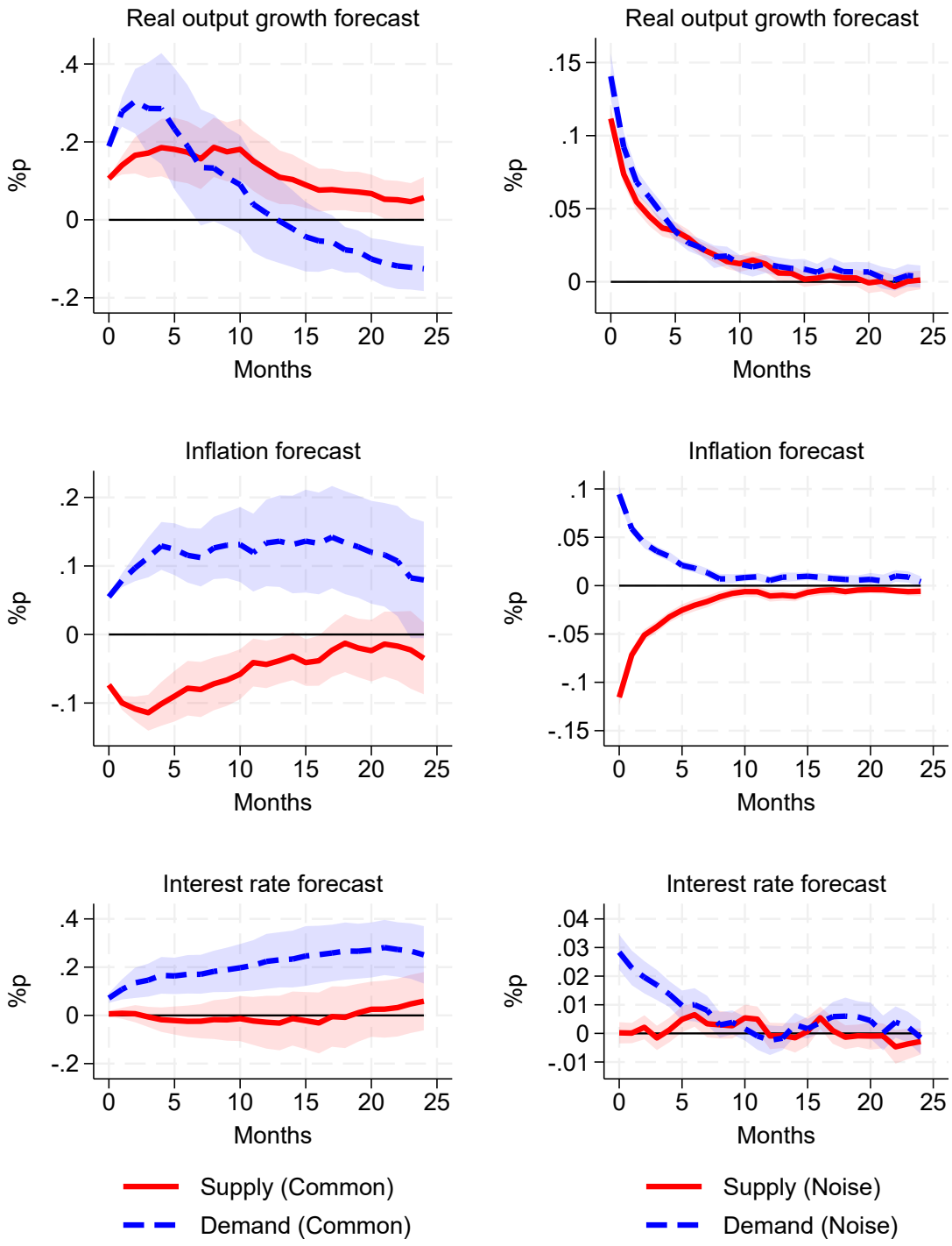

Figure 6: Impulse response functions of Macroeconomic Forecasts to Common Belief and Noise Shocks.

Notes: This figure shows the impulse response functions of forecasts to common belief and noise shocks. The left and right columns report responses to the common belief and noise shocks, respectively. The shaded areas are 90% confidence bands computed from the Driscoll and Kraay (1998) standard errors.

$\mathbb{VAR}_t$ and $\mathbb{COV}_t$ denote the cross-sectional variance and covariance across forecasters i conditional on each time point t. The terms (a)-(e) correspond to the contributions of each component to disagreement, as measured by the covariance of each component with the actual forecasts ($\mathbb{F}_{it}[x_{t+h}]$). Specifically, the term (a) represents the contribution of individual anchors to disagreement, while terms (b) and (c) capture the contribution of common belief supply and demand shocks to disagreement. Since the rotations in Section 3.3 leave the common component unchanged, the sum of (b) and (c) does not depend on the sign restrictions. Only its split into supply and demand does. On the other hand, terms (d) and (e) represent the contribution of idiosyncratic supply and demand noise shocks to disagreement. An alternative interpretation would be that the sum of (b) and (d) corresponds to supply-side disagreement and the sum of (c) and (e) represents demand-side disagreement.

4.2.2 Historical Decomposition

Figure 7 provides the historical decomposition of disagreement about real output growth (left panels) and inflation (right panels) forecasts based on equation (18). The decomposition is conducted along two dimensions: Common vs Noise (upper panels) and Supply vs Demand (lower panels). Common is the sum of contributions from common belief supply and demand shocks, whereas Noise is the sum of contributions from idiosyncratic supply and demand noise shocks. Similarly, the Supply and Demand categories lump the contributions from supply- and demand-type shocks, respectively. These components, along with the contribution from the anchors (purple), sum up to the observed disagreement, the cross-sectional variance across forecasters.[27]

To complement the visual analysis, the percentage contribution of each component in equation (18) is calculated by dividing each term on the right-hand side by the left-hand side, with the results presented in Table 4. Panels A and B display the percentage contribution to disagreement about real output growth and inflation forecasts, respectively. The percentages are averaged over different time periods. On the right half of the table, the contributions of the shocks are also categorized for easier comparison. The 'Common' and 'Noise' columns combine the contributions from common belief shocks (C.S. + C.D.) and noise shocks (S.N. + D.N.), respectively. Similarly, the 'Supply' and 'Demand' columns lump the contributions from supply shocks (C.S. + S.N.) and demand shocks (C.D. + D.N.), respectively.

First of all, the historical decomposition highlights the predominant role of idiosyncratic noise shocks in explaining disagreement among forecasters. This is evident from the upper

[27]Since the individual fixed effect does not vary over time, its contribution varies through changes in the composition of forecasters in each survey round and through its covariance with the other components of the forecasts.

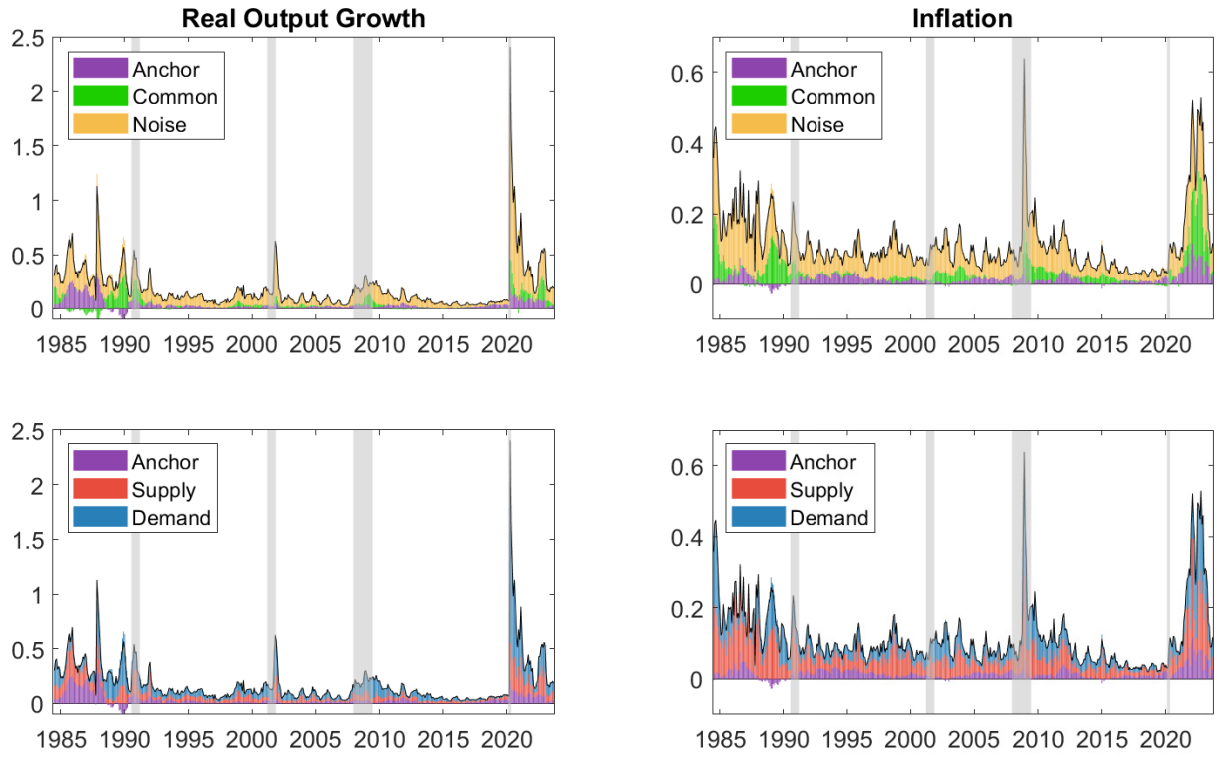

Figure 7: Historical Decomposition of Disagreement

Notes: The figure displays the historical contribution of each component to the disagreement about real output growth (left) and inflation (right) into common belief and noise shocks (upper panel) and supply and demand shocks (lower panel). The gray-shaded areas indicate NBER recessions.

panels in Figure 7 that a substantial portion of the areas under disagreement about real output growth and inflation is filled with contributions from noise shocks (yellow). This impression is also reinforced by the combined contribution of noise shocks which is about 70% to the disagreement (Table 4, Col. Noise). This implies that information dispersion due to noise shocks is the major source of forecast disagreement.

Second, the green areas in the upper panels of Figure 7 illustrate that common belief shocks tend to contribute to disagreement more periodically, with an interesting difference between the two variables. Table 4, Col. Common reveals that common belief shocks are more relevant for the countercyclicality of disagreement about real output growth compared to inflation. For growth, the contribution is around 8.4% in non-recessionary periods, increasing to approximately 20% during recessions. This implies that the significance of non-information heterogeneity, such as the level of attention, is state-dependent, consistent with the empirical evidence on the countercyclicality of attention (Song and Stern, 2025; Flynn and K. Sastry, 2024). In contrast, the contribution to inflation disagreement is more

Table 4: Contribution to Disagreement

	Sum	Anchor	C.S.	C.D.	S.N.	D.N.	Common	Noise	Supply	Demand
A. Real output growth										
Full sample	100	19.6	4.0	5.4	28.5	42.5	9.4	71.0	32.5	47.9
(±1 s.e.)		[17.7, 21.5]	[3.2, 4.8]	[4.2, 6.6]	[25.6, 31.4]	[39.5, 45.5]				
Non-Recession	100	20.1	3.9	4.5	29.1	42.3	8.4	71.5	33.1	46.8
Recession	100	14.0	5.0	14.9	21.9	44.2	19.9	66.1	26.9	59.1
1984M7-1999	100	19.5	6.5	5.2	28.2	40.6	11.8	68.7	34.7	45.8
2000-2023M9	100	19.6	2.4	5.5	28.8	43.7	7.9	72.5	31.1	49.2
B. Inflation										
Full sample	100	15.8	4.9	9.9	41.2	28.2	14.8	69.4	46.1	38.2
(±1 s.e.)		[14.2, 17.3]	[4.3, 5.5]	[8.9, 11.0]	[38.6, 43.7]	[25.7, 30.8]				
Non-Recession	100	16.2	5.0	9.8	40.7	28.3	14.8	69.0	45.7	38.1
Recession	100	11.3	3.9	11.4	45.7	27.8	15.3	73.4	49.5	39.2
1984M7-1999	100	14.2	8.1	6.4	42.0	29.3	14.5	71.2	50.1	35.7
2000-2023M9	100	16.8	2.8	12.2	40.6	27.6	15.0	68.2	43.4	39.8

Notes: The left half of the table displays the percentage contribution of each component in equation (18) to disagreement. To calculate the contribution at each time point, each component is divided by the total disagreement ($\mathbb{VAR}_t[\mathbb{F}_{it}[x_{t+h}]]$). The percentage contributions are then averaged over the full sample, non-recession periods, and recession periods. The right half of the table categorizes the contribution of shocks by type. Columns Common and Noise are the sum of common belief (C.S. + C.D.) and noise (S.N. + D.N.) shocks, respectively. Columns Supply and Demand lump supply (C.S. + S.N.) and demand (C.D. + D.N.) shocks, respectively. Panel A presents the contribution to disagreement about real output growth forecasts, while Panel B presents the contribution to disagreement regarding inflation forecasts. The contributions are calculated considering a one-month lag in the publication of the survey. Bracketed entries beneath the full-sample rows are one-standard-error bands for the decomposition shares, computed from the bootstrap described in Appendix E.3.

stable at around 15% regardless of the state of the economy.

Third, individual anchors on average account for about 10-20% of disagreement about real output growth and inflation. Visual analysis shows that the contribution of the anchors (purple) is relatively more pronounced during the 1980s and the 2020s. These are periods in which real output growth and inflation exhibited high volatility and trends. This may suggest that differences in the perceived long-run levels across forecasters matter more when macroeconomic variables exhibit heightened volatility and trends.

Lastly, the decomposition into supply and demand provides deeper insights into the sources of disagreement. A comparison of the 'Supply' and 'Demand' columns reveals that disagreement about real output growth is primarily demand-driven (47.9%), including both demand noise shocks and common belief demand shocks. In contrast, inflation disagreement is largely attributable to supply-side factors (46.1%), predominantly supply noise shocks (41.2%). This suggests that while information dispersion is the main driver of disagreement for both variables, the nature of the dispersed information could be different. Inflation disagreement is more sensitive to supply-side information, whereas real output growth disagreement is shaped by demand-side information. Additionally, supply-side influences were particularly pronounced during the 1980s and 1990s, especially for inflation. The last two columns of Table 4 show that the supply-side contribution to disagreement has declined from 34.7% to 31.1% for real output growth and from 50.1% to 43.4% for inflation.

Table 5: Contribution to Disagreement by Historical Episodes

	Sum	Anchor	C.S.	C.D.	S.N.	D.N.	Common	Noise	Supply	Demand
A. Real output growth										
Recession										
Gulf War	100	17.4	19.2	17.1	20.2	26.2	36.3	46.3	39.4	43.2
Dotcom	100	13.1	-3.4	7.0	20.8	62.6	3.6	83.4	17.4	69.6
Financial Crisis	100	12.0	2.9	18.7	23.1	43.3	21.5	66.4	26.0	62.0
Covid-19	100	19.2	1.4	8.1	22.3	49.0	9.5	71.3	23.6	57.1
Non-Recession										
Post-pandemic Inflation	100	19.7	6.1	15.9	26.3	32.0	22.0	58.3	32.4	47.9
B. Inflation										
Recession										
Gulf War	100	10.2	12.3	10.2	46.5	20.8	22.5	67.2	58.8	31.0
Dotcom	100	6.7	2.7	9.6	42.0	39.0	12.3	81.0	44.6	48.7
Financial Crisis	100	12.4	0.3	12.4	48.4	26.5	12.7	74.9	48.7	38.9
Covid-19	100	21.2	5.1	13.6	36.8	23.3	18.7	60.1	41.9	36.9
Non-Recession										
Post-pandemic Inflation	100	20.9	8.1	22.0	30.0	19.1	30.1	49.1	38.1	41.0

Notes: The left half of the table displays the percentage contribution of each component in equation (18) to disagreement. To calculate the contribution at each time point, each component is divided by the total disagreement ($\mathbb{VAR}_t[\mathbb{F}_{it}[x_{t+h}]]$). The percentage contributions are then averaged over the months of each episode. The right half of the table categorizes the contribution of shocks by type. Columns Common and Noise are the sum of common belief (C.S. + C.D.) and noise (S.N. + D.N.) shocks, respectively. Columns Supply and Demand lump supply (C.S. + S.N.) and demand (C.D. + D.N.) shocks, respectively. Panel A presents the contribution to disagreement about real output growth forecasts, while Panel B presents the contribution to disagreement regarding inflation forecasts. The contributions are calculated considering a one-month lag in the publication of the survey. The post-pandemic inflation episode (2021M3–2023M9) includes the Russia-Ukraine War period.

Breakdown of disagreement in historical episodes. To further investigate the time-varying drivers of disagreement, the analysis now turns to disagreement during historical U.S. episodes. In addition to the four recessions in the sample, the post-pandemic inflation surge is also explored. The relative contributions are reported in Table 5, and the episodes are discussed below by the source of disagreement that stands out.

The Gulf War recession (1990M7–1991M3) stands out for the contribution of common belief shocks to the disagreement. These shocks account for 36.3% of growth disagreement and 22.5% of inflation disagreement, compared with 9.4% and 14.8% in the full sample. The recession was closely tied to the war. After August 1990, oil prices doubled within three months (Hamilton, 2013). The drop in consumer confidence and subsequent contraction in spending were difficult to explain based on economic fundamentals alone (Blanchard, 1993; R. E. Hall, 1993; Walsh, 1993). In other words, the outbreak of the war was a clear shock, but its macroeconomic propagation mechanism was not. This episode illustrates how large and salient disruptions can generate heterogeneous interpretations among forecasters, thereby contributing to disagreement.

In contrast, noise shocks were the dominant source of disagreement during the Dot-com recession (2001M3–2001M11), the Global Financial Crisis (GFC, 2007M12–2009M6) and

the Covid-19 recession (2020M2–2020M4). They account for 83.4%, 66.4% and 71.3% of growth disagreement and 81.0%, 74.9% and 60.1% of inflation disagreement. All of these downturns featured significant real-time uncertainty. The Dot-com recession is characterized by heightened volatility in asset prices, consistent with the heterogeneous beliefs behind the trading volume of the Dot-com period (Scheinkman and Xiong, 2003). The GFC featured a severe credit crunch and a collapse in consumer and business spending, which triggered a deep recession. The Covid-19 recession was an unprecedented event, followed by the disruption of supply chains and lockdowns. These show that when a downturn features real-time or financial uncertainty, the disagreement mainly reflects dispersed information.

The post-pandemic inflation surge (2021M3–2023M9) was also characterized by multiple disturbances, including supply chain disruptions, fiscal stimulus, pent-up demand, and the energy price shock following Russia's invasion of Ukraine. Similar to the Gulf War recession, common belief shocks account for a substantial share (30.1%) of inflation disagreement, mostly through demand rather than supply (22.0% vs. 8.1%). Every forecaster observed the news about fiscal stimulus, pent-up demand and monetary policy, but the assessment of how much it mattered for inflation could differ across their subjective models. Moreover, supply noise shocks also made a large contribution, accounting for 30.0% of disagreement, compared with 19.1% for demand noise shocks. This finding is consistent with the debate at that time over whether adverse supply shocks would prove transitory or persistent, a problem that was difficult to assess in real time. This episode illustrates that inflation disagreement reflected both heterogeneous assessments of demand-side news and dispersed information about the nature of supply shocks.

Summary. Overall, the historical decomposition points out both unconditional and conditional sources of disagreement. Unconditionally, the main contributors are idiosyncratic noise shocks. However, the relative influence of each source varies over time, as further evidenced by the supply and demand, and historical decompositions.

The decomposition has implications for the existing theories of expectation formation. One is that the dominant role of idiosyncratic noise shocks, which account for about 70% of disagreement, supports noisy information models in which agents observe idiosyncratic signals (Woodford, 2003; Sims, 2003; Coibion and Gorodnichenko, 2012; Coibion and Gorodnichenko, 2015).

The other is the role of heterogeneous loadings on common shocks. The heterogeneous loadings may capture different subjective models or heterogeneous degrees of attention or forecasting abilities. Although their contribution is smaller than that of the noise shocks, common belief shocks exhibit non-trivial state-dependent contribution to disagreement and

persistent responses of beliefs to the shocks. The results suggest that while information dispersion is the main source of disagreement, state-dependence or persistence of disagreement which arises from heterogeneous anchors or heterogeneous subjective models is also a key feature of expectation formation.

5 Discussions and Robustness

This section presents discussions and robustness checks regarding the empirical results. In-depth explanations and relevant results are provided in Appendix E as needed.

Interest rate forecasts In modern macroeconomics, the evolution of output and inflation is typically considered jointly with monetary policy since central banks stabilize output and inflation using interest rate policies. The baseline analysis does not include the interest rate forecast as it makes the identification of supply and demand noise shocks more computationally challenging by substantially increasing the number of moment conditions to consider. In Appendix E.1, the disagreement decomposition into anchors, heterogeneous responses to common belief shocks, and noise shocks is reported. The results drawn in previous sections regarding output growth and inflation disagreement are not substantially affected by the inclusion of interest rate forecasts.

Conventional Sign Restriction Identification The rationale for opting for higher-order moment identification over the conventional sign restriction approach lies in the limitation of the latter, which only offers set identification. Appendix E.2 illustrates how the decomposition of disagreement depends on the researcher's choice within the set. Depending on the specific choice made, either supply or demand noise shocks can be identified as the predominant sources of disagreement.

Inference Estimation uncertainty is assessed by bootstrapping. Appendix E.3 provides the bootstrapping procedure and two sets of results. At the parameter level, most forecasters retain statistically significant loadings ($\mathbf{\Phi}_i$) at the 10% level. More importantly, Table E.4 reports one-standard-error bands for the decomposition shares themselves; the full-sample bands are reproduced in Table 4. The bands indicate that the relative ranking of the sources, in particular the dominance of noise shocks, is statistically stable across bootstrap replications.

Impulse responses of macroeconomic variables Complementing the expectation-level evidence of Section 4.1, Appendix E.4 estimates the impulse responses of monthly macroeconomic variables (CPI, industrial production, employment, the unemployment rate, and the federal funds rate) to the identified common belief supply and demand shocks. The responses align with conventional intuition, with the responses to supply shocks being more

persistent.

VAR lag length This study employs VAR models at both aggregate and individual levels to decompose disagreements. Recognizing that lag number selection may influence the results, the robustness to varying lag lengths is tested in Appendix E.5. It turns out that altering the number of lags in the identification of both common belief shocks and idiosyncratic noise shocks does not have a substantial impact.

Threshold For the stability of individual optimization to identify noise shocks, the baseline analysis only used forecasters that have at least 5 years of participation (60 observations). This threshold inevitably eliminates several forecasters, affecting the composition of the data and hence, the decomposition of disagreement. To check the sensitivity of the empirical result to the choice of the threshold, different values of the threshold are tested. To conserve space, only one representative case is reported in Table E.7. It presents the disagreement decomposition when the threshold is lowered to 40. This threshold leaves few degrees of freedom for an optimization routine that identifies six parameters. Nonetheless, the decomposition result does not change substantially from the original result.

Moment conditions The identification of idiosyncratic noise shocks in this study uses higher-order moments. To ensure the robustness of the result in the subset of moment conditions used for each forecaster, the results using different moment selection criteria are reported in Appendix E.7. The results are basically unaltered from the baseline outcome, validating the initial results.

Number of factors The baseline uses two common factors. Appendix E.8 shows that allowing three factors modestly increases the share attributed to common belief shocks, as expected. Nevertheless, idiosyncratic noise remains the dominant contributor to disagreement, consistently accounting for more than half of the total dispersion in both variables across all periods.

6 Conclusion

This study quantifies the sources of disagreement among professional forecasters using a multivariate factor model that can be easily traced back to the noisy information model. The model provides a historical decomposition of disagreement into three sources: individual anchors (long-run mean), heterogeneous responses to common belief shocks, and idiosyncratic noise shocks.

Application to the Blue Chip survey of professional forecasters uncovers several intriguing findings. First, unconditionally, the most significant source of disagreement is idiosyncratic noise shocks, which, on average, account for more than half of the disagreements observed

in the data. This implies that information dispersion is the major source of disagreement. Second, common belief shocks, which reflect non-information heterogeneity, play a larger role in the countercyclical nature of disagreement regarding real output growth. Third, individual anchors, which mainly reflect heterogeneous perceived long-run levels, make a non-trivial contribution that tends to be larger in periods of heightened volatility. These results suggest that dispersed information, as well as other types of heterogeneity, are important sources of disagreement.

Furthermore, the common belief and idiosyncratic noise shocks are classified into supply and demand types, which adds an additional dimension to understanding forecaster disagreement. Notably, real output growth disagreement is more affected by demand-noise shocks, whereas inflation disagreement is predominantly driven by supply-noise shocks. This finding suggests that although information dispersion is the main driver of disagreement, the particular nature of information which agents disagree about differs across economic variables.

In sum, this paper offers a comprehensive understanding of disagreement using a framework that can be readily mapped back to the standard imperfect information model. It identifies both the unconditional and conditional sources of disagreement, uncovering the different dynamics behind the scenes of each disagreement episode.

Declaration of generative AI: During the preparation of this work, the author(s) used ChatGPT and Claude AI for assistance with writing and coding. The author(s) reviewed and edited the output as needed and take full responsibility for the content of the published article.

References

Ahn, Hie Joo and Leland E Farmer (2024). *Disagreement About the Term Structure of Inflation Expectations*. Finance and Economics Discussion Series 2024-084. Board of Governors of the Federal Reserve System.

Altonji, Joseph G and Lewis M Segal (1996). "Small-sample bias in GMM estimation of covariance structures". In: *Journal of Business & Economic Statistics* 14.3, pp. 353–366.

Andrade, Philippe, Richard K Crump, et al. (2016). "Fundamental disagreement". In: *Journal of Monetary Economics* 83, pp. 106–128.

Andrade, Philippe and Hervé Le Bihan (2013). "Inattentive professional forecasters". In: *Journal of Monetary Economics* 60.8, pp. 967–982.

Andre, Peter et al. (2022). "Subjective models of the macroeconomy: Evidence from experts and representative samples". In: *The Review of Economic Studies* 89.6, pp. 2958–2991.

Andrews, Donald WK and Biao Lu (2001). "Consistent model and moment selection procedures for GMM estimation with application to dynamic panel data models". In: *Journal of econometrics* 101.1, pp. 123–164.

Angeletos, George-Marios, Zhen Huo, and Karthik A Sastry (2021). "Imperfect macroeconomic expectations: Evidence and theory". In: *NBER Macroeconomics Annual* 35.1, pp. 1–86.

Angeletos, George-Marios and Jennifer La'O (2013). "Sentiments". In: *Econometrica* 81.2, pp. 739–779.

Angeletos, George-Marios and Jennifer La'o (2010). "Noisy business cycles". In: *NBER Macroeconomics Annual* 24.1, pp. 319–378.

— (2020). "Optimal monetary policy with informational frictions". In: *Journal of Political Economy* 128.3, pp. 1027–1064.

Bai, Jushan (2003). "Inferential theory for factor models of large dimensions". In: *Econometrica* 71.1, pp. 135–171.

— (2009). "Panel data models with interactive fixed effects". In: *Econometrica* 77.4, pp. 1229–1279.

Bauer, Michael D, Carolin E Pflueger, and Adi Sunderam (2024). "Perceptions about monetary policy". In: *The Quarterly Journal of Economics* 139.4, pp. 2227–2278.

Bekaert, Geert, Eric Engstrom, and Andrey Ermolov (2021). "Identifying aggregate demand and supply shocks using sign restrictions and higher-order moments". In: *Columbia Business School Research Paper*.

Blachard, O and D Quah (1989). "The dynamic effects of aggregate supply and demand shocks". In: *American Economic Review* 79.4, pp. 655–673.

Blanchard, Olivier (1993). "Consumption and the Recession of 1990-1991". In: *The American Economic Review* 83.2, pp. 270–274.

Bordalo, Pedro et al. (2020). "Overreaction in macroeconomic expectations". In: *American Economic Review* 110.9, pp. 2748–82.

Bray, Margaret M and Nathan E Savin (1986). "Rational expectations equilibria, learning, and model specification". In: *Econometrica: Journal of the Econometric Society*, pp. 1129–1160.

Broer, Tobias and Alexandre N Kohlhas (2022). "Forecaster (mis-) behavior". In: *Review of Economics and Statistics*, pp. 1–45.

Capistrán, Carlos and Allan Timmermann (2009). "Disagreement and biases in inflation expectations". In: *Journal of Money, Credit and Banking* 41.2-3, pp. 365–396.

Carlin, Bruce I, Francis A Longstaff, and Kyle Matoba (2014). "Disagreement and asset prices". In: *Journal of Financial Economics* 114.2, pp. 226–238.

Clements, Michael P (2018). "Do macroforecasters herd?" In: *Journal of Money, Credit and Banking* 50.2-3, pp. 265–292.

Coibion, Olivier and Yuriy Gorodnichenko (2012). "What can survey forecasts tell us about information rigidities?" In: *Journal of Political Economy* 120.1, pp. 116–159.

— (2015). "Information rigidity and the expectations formation process: A simple framework and new facts". In: *American Economic Review* 105.8, pp. 2644–2678.

Coibion, Olivier, Yuriy Gorodnichenko, and Tiziano Ropele (2023). *Inflation Expectations and Misallocation of Resources: Evidence from Italy*. Tech. rep. National Bureau of Economic Research.

Crump, Richard K, Stefano Eusepi, and Emanuel Moench (2024). "Is There Hope for the Expectations Hypothesis?" In: *FRB of New York Staff Report* 1098.

Crump, Richard K, Stefano Eusepi, Emanuel Moench, and Bruce Preston (2023). "The term structure of expectations". In: *Handbook of Economic Expectations*. Elsevier, pp. 507–540.

Dovern, Jonas (2015). "A multivariate analysis of forecast disagreement: Confronting models of disagreement with survey data". In: *European Economic Review* 80, pp. 16–35.

Dovern, Jonas, Ulrich Fritsche, and Jiri Slacalek (2012). "Disagreement among forecasters in G7 countries". In: *Review of Economics and Statistics* 94.4, pp. 1081–1096.

Driscoll, John C and Aart C Kraay (1998). "Consistent covariance matrix estimation with spatially dependent panel data". In: *Review of economics and statistics* 80.4, pp. 549–560.

Falck, Elisabeth, Mathias Hoffmann, and Patrick Hürtgen (2021). "Disagreement about inflation expectations and monetary policy transmission". In: *Journal of Monetary Economics* 118, pp. 15–31.

Flynn, Joel P and Karthik Sastry (2024). *Attention cycles*. Tech. rep. National Bureau of Economic Research.

Ganics, Gergely, Barbara Rossi, and Tatevik Sekhposyan (2024). "From fixed-event to fixed-horizon density forecasts: Obtaining measures of multihorizon uncertainty from survey density forecasts". In: *Journal of Money, Credit and Banking* 56.7, pp. 1675–1704.

Gemmi, Luca and Rosen Valchev (2023). "Biased Surveys". In: *Working Paper*.

Giacomini, Raffaella, Vasiliki Skreta, and Javier Turen (2020). "Heterogeneity, inattention, and bayesian updates". In: *American Economic Journal: Macroeconomics* 12.1, pp. 282–309.

Hall, Peter and Joel L Horowitz (1996). "Bootstrap critical values for tests based on generalized-method-of-moments estimators". In: *Econometrica: Journal of the Econometric Society*, pp. 891–916.

Hall, Robert E (1993). "Macro Theory and the Recession of 1990-1991". In: *The American Economic Review* 83.2, pp. 275–279.

Hamilton, James D (2013). "Historical oil shocks". In: *Routledge Handbook of Major Events in Economic History*. Routledge, pp. 239–265.

Herbst, Edward and Fabian Winkler (2026). "The Factor Structure of Disagreement". In: *Journal of Business & Economic Statistics* 44.2, pp. 677–690.

Hou, Chenyu and Tao Wang (2025). *Uncovering Subjective Models from Survey Expectations*. Staff Working Paper 2025-31. Bank of Canada.

Johnson, David R (2002). "The effect of inflation targeting on the behavior of expected inflation: evidence from an 11 country panel". In: *Journal of Monetary Economics* 49.8, pp. 1521–1538.

Jordà, Òscar (2005). "Estimation and inference of impulse responses by local projections". In: *American economic review* 95.1, pp. 161–182.

Juodis, Artūras and Simas Kučinskas (2023). "Quantifying noise in survey expectations". In: *Quantitative Economics* 14.2, pp. 609–650.

Kim, Husang (2026). *The Perceived Monetary Policy Rule: Identification and Macroeconomic Implications*. Working Paper 6171027. SSRN.

Lahiri, Kajal and Xuguang Sheng (2008). "Evolution of forecast disagreement in a Bayesian learning model". In: *Journal of Econometrics* 144.2, pp. 325–340.

Lorenzoni, Guido (2009). "A theory of demand shocks". In: *American economic review* 99.5, pp. 2050–2084.

Mankiw, N Gregory and Ricardo Reis (2002). "Sticky information versus sticky prices: a proposal to replace the New Keynesian Phillips curve". In: *The Quarterly Journal of Economics* 117.4, pp. 1295–1328.

Marcet, Albert and Thomas J Sargent (1989). "Convergence of least squares learning mechanisms in self-referential linear stochastic models". In: *Journal of Economic theory* 48.2, pp. 337–368.

Marinovic, Iván, Marco Ottaviani, and Peter Sorensen (2013). "Forecasters' objectives and strategies". In: *Handbook of economic forecasting*. Vol. 2. Elsevier, pp. 690–720.

Miller, Edward M (1977). "Risk, uncertainty, and divergence of opinion". In: *The Journal of finance* 32.4, pp. 1151–1168.

Montiel Olea, José Luis, Mikkel Plagborg-Møller, and Eric Qian (2022). "SVAR Identification From Higher Moments: Has the Simultaneous Causality Problem Been Solved?" In: *AEA*

Papers and Proceedings. Vol. 112. American Economic Association 2014 Broadway, Suite 305, Nashville, TN 37203, pp. 481–485.

Patton, Andrew J and Allan Timmermann (2010). "Why do forecasters disagree? Lessons from the term structure of cross-sectional dispersion". In: *Journal of Monetary Economics* 57.7, pp. 803–820.

Rich, Robert and Joseph Tracy (2021). "A closer look at the behavior of uncertainty and disagreement: Micro evidence from the euro area". In: *Journal of Money, Credit and Banking* 53.1, pp. 233–253.

Ryngaert, Jane (2017). "What Do (and Don't) Forecasters Know About US Inflation?" In: *Journal of Money, Credit and Banking*.

Scanlan, Susannah (2023). "Attention Allocation and the Factor Structure of Forecasts". In.

Scheinkman, Jose A and Wei Xiong (2003). "Overconfidence and speculative bubbles". In: *Journal of political Economy* 111.6, pp. 1183–1220.

Siklos, Pierre L (2013). "Sources of disagreement in inflation forecasts: An international empirical investigation". In: *Journal of International Economics* 90.1, pp. 218–231.

Sims, Christopher A (2003). "Implications of rational inattention". In: *Journal of monetary Economics* 50.3, pp. 665–690.

Song, Wenting and Samuel Stern (2025). "Firm inattention and the efficacy of monetary policy: A text-based approach". In: *Review of Economic Studies* 92.5, pp. 3438–3469.

Taubinsky, Dmitry et al. (July 2024). *Beliefs About the Economy are Excessively Sensitive to Household-Level Shocks: Evidence from Linked Survey and Administrative Data*. Working Paper 32664. National Bureau of Economic Research. DOI: 10.3386/w32664. URL: http://www.nber.org/papers/w32664.

Uhlig, Harald (2005). "What are the effects of monetary policy on output? Results from an agnostic identification procedure". In: *Journal of Monetary Economics* 52.2, pp. 381–419.

Walsh, Carl E (1993). "What caused the 1990-1991 recession?" In: *Economic Review-Federal Reserve Bank of San Francisco* 2, p. 33.

Woodford, Michael (2003). "Imperfect common knowledge and the effects of monetary policy". In: *Knowledge, Information, and Expectations in Modern Macroeconomics: In Honor of Edmund S. Phelps* 1.1, pp. 25–58.

A Proofs

A.1 Proposition 1

This appendix provides the derivation of the empirical factor model from the recursive forecast formula. The agent is assumed to report $\mathbb{F}_{it}[\mathbf{x}_{t+1}]$:

$$\mathbb{F}_{it}[\mathbf{x}_{t+1}] - \boldsymbol{\mu}_i = \mathbf{A}_i \left\{ \mathbf{G}_i \left(\mathbf{s}_{it} - \boldsymbol{\mu}_i \right) + \left(\mathbf{I} - \mathbf{G}_i \right) \left(\mathbb{F}_{it-1}[\mathbf{x}_t] - \boldsymbol{\mu}_i \right) \right\} \tag{19}$$

Iterating the forecast equation (19) reveals the underlying factor structure:

$$\begin{aligned}
\mathbb{F}_{it}[\mathbf{x}_{t+1}] - \boldsymbol{\mu}_i =& \mathbf{A}_i \left\{ \mathbf{G}_i \left(\mathbf{s}_{it} - \boldsymbol{\mu}_i \right) + \left(\mathbf{I} - \mathbf{G}_i \right) \left(\mathbb{F}_{it-1}[\mathbf{x}_t] - \boldsymbol{\mu}_i \right) \right\} \\
=& \sum_{k=0}^{\infty} \Big(\mathbf{A}_i (\mathbf{I} - \mathbf{G}_i) \Big)^k \mathbf{A}_i \mathbf{G}_i \left(\mathbf{s}_{it-k} - \boldsymbol{\mu}_i \right) \\
=& \sum_{k=0}^{\infty} \Big(\mathbf{A}_i (\mathbf{I} - \mathbf{G}_i) \Big)^k \mathbf{A}_i \mathbf{G}_i \left(\boldsymbol{\mu} - \boldsymbol{\mu}_i \right) + \sum_{k=0}^{\infty} \Big(\mathbf{A}_i (\mathbf{I} - \mathbf{G}_i) \Big)^k \mathbf{A}_i \mathbf{G}_i \left(\mathbf{x}_{t-k} - \boldsymbol{\mu} \right) \\
&+ \sum_{k=0}^{\infty} \Big(\mathbf{A}_i (\mathbf{I} - \mathbf{G}_i) \Big)^k \mathbf{A}_i \mathbf{G}_i \mathbf{w}_{it-k}
\end{aligned}$$

Using $\mathbf{x}_{t-k} - \boldsymbol{\mu} = \mathbf{B}\boldsymbol{\epsilon}_{\boldsymbol{t-k}} + \mathbf{AB}\boldsymbol{\epsilon}_{\boldsymbol{t-k-1}} + \mathbf{A}^2\mathbf{B}\boldsymbol{\epsilon}_{\boldsymbol{t-k-2}} + \cdots$

$$\begin{aligned}
\mathbb{F}_{it}[\mathbf{x}_{t+1}] - \boldsymbol{\mu}_i =& \sum_{k=0}^{\infty} \Big(\mathbf{A}_i (\mathbf{I} - \mathbf{G}_i) \Big)^k \mathbf{A}_i \mathbf{G}_i \left(\boldsymbol{\mu} - \boldsymbol{\mu}_i \right) \\
&+ \sum_{k=0}^{\infty} \Big(\mathbf{A}_i (\mathbf{I} - \mathbf{G}_i) \Big)^k \mathbf{A}_i \mathbf{G}_i \Big(\mathbf{B}\boldsymbol{\epsilon}_{\boldsymbol{t-k}} + \mathbf{AB}\boldsymbol{\epsilon}_{\boldsymbol{t-k-1}} + \mathbf{A}^2\mathbf{B}\boldsymbol{\epsilon}_{\boldsymbol{t-k-2}} + \cdots \Big) \\
&+ \sum_{k=0}^{\infty} \Big(\mathbf{A}_i (\mathbf{I} - \mathbf{G}_i) \Big)^k \mathbf{A}_i \mathbf{G}_i \mathbf{w}_{it-k}
\end{aligned}$$

This can be rewritten as

$$\mathbb{F}_{it}[\mathbf{x}_{t+1}] = \mathbf{b}_i + \sum_{k=0}^{\infty} \boldsymbol{\lambda}_{i,k} \boldsymbol{\epsilon}_{t-k} + \mathbf{v}_{it}$$

where

$$\mathbf{b}_i = \boldsymbol{\mu}_i + \Big(\mathbf{I} - \mathbf{A}_i(\mathbf{I} - \mathbf{G}_i)\Big)^{-1} \mathbf{A}_i \mathbf{G}_i \left(\boldsymbol{\mu} - \boldsymbol{\mu}_i\right)$$
$$\boldsymbol{\lambda}_{i,k} = \sum_{j=0}^{k} \Big(\mathbf{A}_i(\mathbf{I} - \mathbf{G}_i)\Big)^{j} \mathbf{A}_i \mathbf{G}_i \mathbf{A}^{k-j} \mathbf{B}$$
$$\mathbf{v}_{it} = \sum_{k=0}^{\infty} \Big(\mathbf{A}_i(\mathbf{I} - \mathbf{G}_i)\Big)^{k} \mathbf{A}_i \mathbf{G}_i \mathbf{w}_{it-k}$$

The noise can be expressed as a VAR(1) process.

$$\begin{aligned}\mathbf{v}_{it} &= \sum_{k=0}^{\infty} \Big(\mathbf{A}_i(\mathbf{I} - \mathbf{G}_i)\Big)^{k} \mathbf{A}_i \mathbf{G}_i \mathbf{w}_{it-k} \\ &= \boldsymbol{\rho}_i \mathbf{v}_{it-1} + \boldsymbol{\Phi}_i \mathbf{u}_{it}\end{aligned}$$

where

$$\boldsymbol{\rho}_i = \Big(\mathbf{A}_i(\mathbf{I} - \mathbf{G}_i)\Big)$$
$$\boldsymbol{\Phi}_i = \mathbf{A}_i \mathbf{G}_i \boldsymbol{\Sigma}_i$$

Thus, equation (19) can be rewritten as

$$\mathbb{F}_{it}[\mathbf{x}_{t+1}] = \mathbf{b}_i + \sum_{k=0}^{\infty} \boldsymbol{\lambda}_{i,k} \boldsymbol{\epsilon}_{t-k} + \mathbf{v}_{it} \tag{20}$$

■

A.2 Proposition 2

The reduced form contemporaneous loading is

$$\boldsymbol{\lambda}_{i,0} = \mathbf{A}_i \mathbf{G}_i \mathbf{B}$$
$$\boldsymbol{\Phi}_i = \mathbf{A}_i \mathbf{G}_i \boldsymbol{\Sigma}_i$$

Then with $\mathbf{M}_i = \mathbf{A}_i\mathbf{G}_i$ and for some matrix $\mathbf{S} \in \{\mathbf{B}, \mathbf{\Sigma}_i\}$, it suffices to show that the following matrix satisfies the sign restriction:

$$\begin{aligned}\mathbf{M}_i\mathbf{S} &= \begin{bmatrix} M_{11} & M_{12} \\ M_{21} & M_{22} \end{bmatrix} \begin{bmatrix} S_{11} & S_{12} \\ S_{21} & S_{22} \end{bmatrix} \\ &= \begin{bmatrix} M_{11}S_{11} + M_{12}S_{21} & M_{11}S_{12} + M_{12}S_{22} \\ M_{21}S_{11} + M_{22}S_{21} & M_{21}S_{12} + M_{22}S_{22} \end{bmatrix} \\ &= \begin{bmatrix} + & + \\ - & + \end{bmatrix}.\end{aligned}$$

The conditions on the first row imply

$$\begin{cases} -\frac{\mathbf{S}_{12}}{\mathbf{S}_{22}} < \frac{\mathbf{M}_{12}}{\mathbf{M}_{11}} < -\frac{\mathbf{S}_{11}}{\mathbf{S}_{21}} & \text{if } \mathbf{M}_{11} > 0 \\ -\frac{\mathbf{S}_{11}}{\mathbf{S}_{21}} < \frac{\mathbf{M}_{12}}{\mathbf{M}_{11}} < -\frac{\mathbf{S}_{12}}{\mathbf{S}_{22}} & \text{if } \mathbf{M}_{11} < 0 \end{cases}$$

The second condition yields a contradiction because the left side is positive due to $\mathbf{S}_{21} < 0$ whereas the right side is negative. If $\mathbf{M}_{11} = 0$, then $\mathbf{M}_{12}\mathbf{S}_{21} > 0$, which also yields a contradiction. Similarly, the conditions on the second row imply

$$\begin{cases} -\frac{\mathbf{S}_{22}}{\mathbf{S}_{12}} < \frac{\mathbf{M}_{21}}{\mathbf{M}_{22}} < -\frac{\mathbf{S}_{21}}{\mathbf{S}_{11}} & \text{if } \mathbf{M}_{22} > 0 \\ -\frac{\mathbf{S}_{21}}{\mathbf{S}_{11}} < \frac{\mathbf{M}_{21}}{\mathbf{M}_{22}} < -\frac{\mathbf{S}_{22}}{\mathbf{S}_{12}} & \text{if } \mathbf{M}_{22} < 0 \end{cases}$$

The second condition also yields a contradiction because the left side is positive, whereas the right side is negative. Thus, the sign restrictions are compatible with

$$\begin{cases} -\frac{\mathbf{S}_{12}}{\mathbf{S}_{22}} < \frac{\mathbf{M}_{12}}{\mathbf{M}_{11}} < -\frac{\mathbf{S}_{11}}{\mathbf{S}_{21}} & \text{if } \mathbf{M}_{11} > 0 \\ -\frac{\mathbf{S}_{22}}{\mathbf{S}_{12}} < \frac{\mathbf{M}_{21}}{\mathbf{M}_{22}} < -\frac{\mathbf{S}_{21}}{\mathbf{S}_{11}} & \text{if } \mathbf{M}_{22} > 0 \end{cases}$$

which is the condition in the proposition. The sufficiency is straightforward.

■

B Estimation Procedure

B.1 Optimal Number of Factors

To determine the optimal number of factors for the baseline case, the extent to which including additional factors explains the variance in the forecast data is considered. Table B.1

Table B.1: Contribution of Common Factors to Forecasts

	Cumulative variance explained by common factors				
Number of Common Factors:	1	2	3	4	5
A. Real output growth:					
Mean R^2 across forecasters	0.78	0.87	0.90	0.92	0.93
Median R^2 across forecasters	0.86	0.90	0.92	0.94	0.94
B. Inflation:					
Mean R^2 across forecasters	0.17	0.80	0.83	0.86	0.88
Median R^2 across forecasters	0.07	0.86	0.87	0.90	0.91

Notes: The table presents metrics showing the cumulative variance associated with each additional factor. The first two rows display the mean and median R^2 values corresponding to different numbers of factors in the real output growth forecasts of 116 forecasters surveyed by BCEI. The last two rows show the mean and median R^2 values associated with different numbers of factors in the inflation forecasts of the same 116 forecasters.

provides a summary of this metric.

The key finding from this table is that the first two factors explain a significant portion of the output growth and inflation forecasts across the 116 forecasters in the sample. According to the R^2 values, the first common factor heavily focuses on real output growth and leaves most of the inflation forecast unexplained. The second factor then contributes a substantial amount of explanatory power to inflation forecasts, collectively explaining around 80-86% of inflation forecasts.

However, the marginal contribution to the cumulative explained variance by the third factor and subsequent factors is relatively small. The average increase in R^2 achieved by including the third factor is 3% for both variables. Considering that the first two common factors, particularly the first one, account for more than 80% of the variance in the data, two factors are chosen as the baseline case.

B.2 Estimation of Common Factors

To estimate the common factors, loadings, and anchors, this paper employs the iterative least-squares method (Bai, 2003; Bai, 2009). The procedure of estimation outlined below primarily follows Juodis and Kučinskas (2023). The model to be estimated is

$$\mathbb{F}_{it}[\mathbf{x}_{t+h}] = \mathbf{b}_i + \boldsymbol{\lambda}_i^{'}\mathbf{f}_t + \mathbf{v}_{it} \tag{21}$$

for a predetermined number of factors. The procedure is initiated by choosing some initial values for the factors, $\hat{\mathbf{f}}_t^{(0)}$. Then, the factor loadings $\boldsymbol{\lambda}_i = \left[\boldsymbol{\lambda}_i^g \ \boldsymbol{\lambda}_i^\pi\right]$ and anchors $\mathbf{b}_i = \left[b_i^g \ b_i^\pi\right]'$

are estimated by running individual time-series regressions for each target variable separately

$$\mathbb{F}_{it}[g_{t+h}] = b_i^g + \boldsymbol{\lambda}_i^{g\prime}\hat{\mathbf{f}}_t^{(0)} + v_{it}^g \tag{22}$$

$$\mathbb{F}_{it}[\pi_{t+h}] = b_i^\pi + \boldsymbol{\lambda}_i^{\pi\prime}\hat{\mathbf{f}}_t^{(0)} + v_{it}^\pi \tag{23}$$

for each forecaster, $i = 1 \cdots N$ using the time periods when the specific forecaster is active. With the estimated factor loadings ($\hat{\boldsymbol{\lambda}}_i^{(0)}$) and anchors ($\hat{\mathbf{b}_i}^{(0)}$), the factors are updated $\hat{\mathbf{f}}_t^{(1)}$ by running the following cross-sectional regressions

$$\mathbb{F}_{\boldsymbol{it}}[\mathbf{x}_{\boldsymbol{t+h}}] - \hat{\mathbf{b}}_i^{(0)} = \mathbf{f}_t'\hat{\boldsymbol{\lambda}}_i^{(0)} + \mathbf{v}_{it} \tag{24}$$

repeatedly for each time $t = 1 \cdots T$ using only the active forecasters at time t. This procedure is iterated until the change in the sum of squared residuals is below the tolerance level. The procedure is repeated with multiple initial starting factors to locate the global minimum.

B.3 Estimation of individual CMD parameters (Second stage)

1. For each forecaster $i = 1, \cdots, I$, use the residuals from the first stage $(\hat{v}_{it}^g, \hat{v}_{it}^\pi)$ to choose the optimal subset of moment conditions by applying the following criterion of Andrews and Lu (2001).

$$\begin{aligned}
\text{MMSC}_{\text{BIC},i}(b,c) &= J_i(b,c) - (|c| - |b|)\ln(n_i) \\
\text{MMSC}_{\text{AIC},i}(b,c) &= J_i(b,c) - 2(|c| - |b|) \\
\text{MMSC}_{\text{HQIC},i}(b,c) &= J_i(b,c) - Q(|c| - |b|)\ln\ln(n_i)
\end{aligned}$$

   where b and c denote the number of parameters and moment conditions being estimated and used. J_i is the optimized value of the CMD objective function. n_i denotes the sample size of forecaster i.

2. For forecasters whose optimal subset of moment conditions indicates overidentification, generate bootstrap samples and conduct an overidentification test based on P. Hall and Horowitz (1996). Define the following bootstrap statistic

$$J_i^* = n_i\left[\left(\hat{\mathbf{m}}_i^* - \mathbf{m}_i(\boldsymbol{\theta}_i^*) - \left(\hat{\mathbf{m}}_i - \mathbf{m}_i(\hat{\boldsymbol{\theta}}_i)\right)\right)'\widehat{\mathbf{W}}_i^{-1}\left(\hat{\mathbf{m}}_i^* - \mathbf{m}_i(\boldsymbol{\theta}_i^*) - \left(\hat{\mathbf{m}}_i - \mathbf{m}_i(\hat{\boldsymbol{\theta}}_i)\right)\right)\right]$$

   Use the distribution of $\{J_{i,s}^{\text{boot}}\}_{s=1}^S$ to compute the critical value which is the $(S \times \tau)^{\text{th}}$ largest value of the distribution. The test rejects the null if the test statistic J_i is larger

than the critical value.

3. Given the subset of moment conditions for each forecaster $i = 1, \cdots, I$, proceed with the minimum distance estimation.

B.4 Higher-order moments

Consider a bivariate system of real GDP growth (g_t) and inflation (π_t). Denote the errors of the VAR model using e^x_{it}, where $x \in \{g, \pi\}$; consistent with equation (12) in the main text, these errors are a linear function of supply and demand noise shocks.

$$e^g_{it} = \phi_{gs} u^s_{it} + \phi_{gd} u^d_{it}$$
$$e^\pi_{it} = -\phi_{\pi s} u^s_{it} + \phi_{\pi d} u^d_{it}$$

The noise shocks are assumed to be independent with mean zero and unit variance. The parameters are assumed to be positive so that the signs of coefficients adhere to the convention. The forecaster-specific subscript i is omitted from the parameters for brevity.

1. Variance of e^g_{it}:

$$\mathbb{VAR}(e^g_{it}) = \mathbb{E}[(e^g_{it})^2] = \phi^2_{gs} + \phi^2_{gd}$$

2. Variance of e^π_{it}:

$$\mathbb{VAR}(e^\pi_{it}) = \mathbb{E}[(e^\pi_{it})^2] = \phi^2_{\pi s} + \phi^2_{\pi d}$$

3. Covariance between e^g_{it} and e^π_{it}

$$\mathbb{COV}(e^g_{it}, e^\pi_{it}) = \mathbb{E}[e^g_{it} e^\pi_{it}] = -\phi_{gs}\phi_{\pi s} + \phi_{gd}\phi_{\pi d}$$

4. Excess Kurtosis of e^g_{it}

$$\mathbb{XK}(e^g_{it}) = \mathbb{E}[(e^g_{it})^4] - 3 = \frac{\phi^4_{gs}(\mathbb{E}[(u^s_{it})^4] - 3) + \phi^4_{gd}(\mathbb{E}[(u^d_{it})^4] - 3)}{(\phi^2_{gs} + \phi^2_{gd})^2}$$

5. Excess Kurtosis of e^π_{it}

$$\mathbb{XK}(e^\pi_{it}) = \mathbb{E}[(e^\pi_{it})^4] - 3 = \frac{\phi^4_{\pi s}(\mathbb{E}[(u^s_{it})^4] - 3) + \phi^4_{\pi d}(\mathbb{E}[(u^d_{it})^4] - 3)}{(\phi^2_{\pi s} + \phi^2_{\pi d})^2}$$

6. Co-excess Kurtosis 1 between e_{it}^g and e_{it}^π

$$\mathbb{COXK}_1(e_{it}^g, e_{it}^\pi) = \mathbb{E}[(e_{it}^g)^3(e_{it}^\pi)] - 3\rho_{g,\pi} = \frac{-\phi_{gs}^3\phi_{\pi s}(\mathbb{E}[(u_{it}^s)^4] - 3) + \phi_{gd}^3\phi_{\pi d}(\mathbb{E}[(u_{it}^d)^4] - 3)}{(\phi_{gs}^2 + \phi_{gd}^2)^{3/2}(\phi_{\pi s}^2 + \phi_{\pi d}^2)^{1/2}}$$

7. Co-excess Kurtosis 2 between e_{it}^g and e_{it}^π

$$\mathbb{COXK}_2(e_{it}^g, e_{it}^\pi) = \mathbb{E}[(e_{it}^g)^2(e_{it}^\pi)^2] - 2\rho_{g,\pi} - 1 = \frac{\phi_{gs}^2\phi_{\pi s}^2(\mathbb{E}[(u_{it}^s)^4] - 3) + \phi_{gd}^2\phi_{\pi d}^2(\mathbb{E}[(u_{it}^d)^4] - 3)}{(\phi_{gs}^2 + \phi_{gd}^2)^{2/2}(\phi_{\pi s}^2 + \phi_{\pi d}^2)^{2/2}}$$

8. Co-excess Kurtosis 3 between e_{it}^g and e_{it}^π

$$\mathbb{COXK}_3(e_{it}^\pi, e_{it}^g) = \mathbb{E}[(e_{it}^g)(e_{it}^\pi)^3] - 3\rho_{g,\pi} = \frac{-\phi_{\pi s}^3\phi_{gs}(\mathbb{E}[(u_{it}^s)^4] - 3) + \phi_{\pi d}^3\phi_{gd}(\mathbb{E}[(u_{it}^d)^4] - 3)}{(\phi_{\pi s}^2 + \phi_{\pi d}^2)^{3/2}(\phi_{gs}^2 + \phi_{gd}^2)^{1/2}}$$

C Identification of Aggregate Shocks based on Realized Data

C.1 Data

This section describes the procedure of identifying the aggregate supply and demand shocks from the realized data of real GDP growth and inflation (GDP deflator). I first obtain the quarterly growth rate of real GDP and GDP deflator from the real-time data of the Federal Reserve Bank of Philadelphia. I transform the data into year-over-year growth rates to align with the Blue Chip forecast data used in the main analysis. For each quarter, I use the first release dataset consistent with the practice in the literature Coibion and Gorodnichenko (2015). The second release is used instead of the missing first release for 1995:Q4.

To align with the horizon format of the Blue Chip forecast data, I compound the quarterly growth rates to transform into the year-over-year rates. The year-over-year series start in 1966:Q3. Figure C.1 shows both transformations together with the consensus forecast.

C.2 Identification using Higher Order Moments

Let $\mathbf{z}_q = (g_q, \pi_q)'$ be the vector of realized growth and inflation data. I estimate by OLS the following VAR with four lags (one year):

$$\mathbf{z}_q = \sum_{l=1}^{p} \mathbf{A}_l \mathbf{z}_{q-l} + \mathbf{\Gamma}'\mathbf{X}_q + \mathbf{e}_q, \qquad \mathbf{e}_q = (e_q^g, e_q^\pi)'. \tag{25}$$

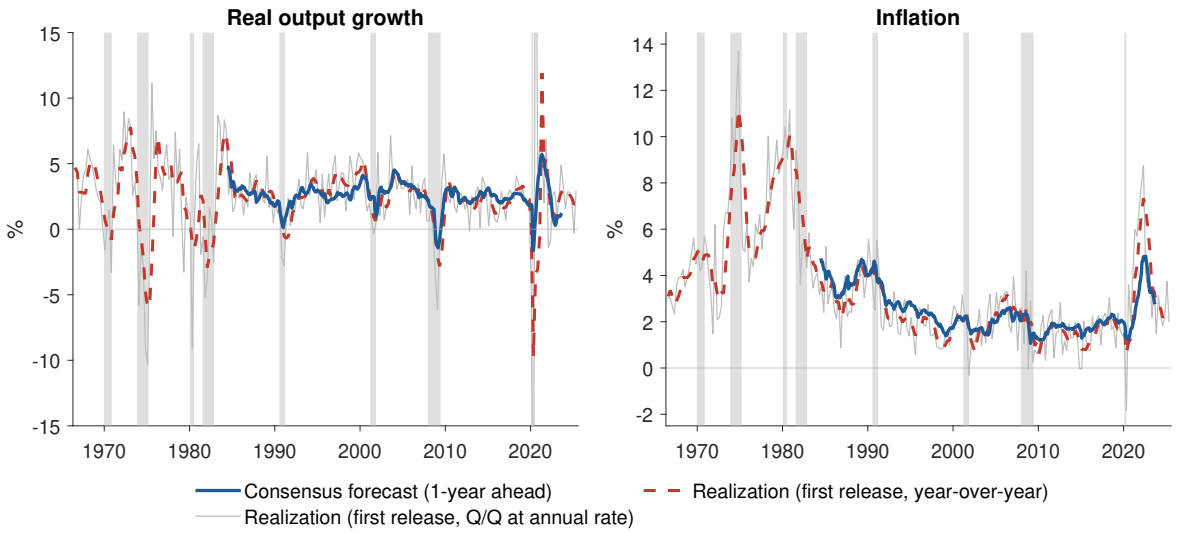

Figure C.1: Consensus forecast and realized data

Notes: One-year-ahead consensus forecast from Blue Chip Economic Indicators (blue, monthly), year-over-year rates used in the VAR (red, dashed) and the original quarterly growth, first-release data (grey). Quarterly values are plotted in the middle month of the quarter. The shaded areas indicate NBER recessions.

$\mathbf{X}_q$ includes a constant and one dummy for each of 2020:Q1, 2020:Q2 and 2021:Q2, to exclude the Covid outliers and the year-over-year base effect of the 2020:Q2 in 2021:Q2. The estimation sample spans 1967:Q3–2025:Q2. The time subscript is written as q to denote quarters, to avoid conflict with the t referring to months in the main text.

As done in the forecaster-level analysis (12), the VAR residuals are assumed to be linear combinations of a supply shock u_q^s and a demand shock u_q^d.

$$e_q^g = \phi^{gs} u_q^s + \phi^{gd} u_q^d, \tag{26}$$

$$e_q^\pi = -\phi^{\pi s} u_q^s + \phi^{\pi d} u_q^d. \tag{27}$$

Here the shocks are assumed to be independent, with zero mean and unit variance. A positive supply shock raises growth and lowers inflation, and a positive demand shock raises both. The loadings are also assumed to be non-negative. The estimation is the same as for the forecasters. I use the higher-order moment based identification via the CMD estimator (13) with identity weighting on the moments of Appendix B.4, computed from the residuals of the non-dummied quarters.

Shocks and estimates. The shocks are recovered from the residuals of every quarter by inverting (26). The shocks for the dummied-out periods are zero by construction. Table C.1 reports the estimates. Based on the estimates of loadings, demand shocks account for

Table C.1: VAR and identification from realized data: estimates

	Full sample
Estimation sample	1967:Q3–2025:Q2
Kurtosis of residual, growth	5.3
Kurtosis of residual, inflation	3.72
ϕ^{gs} (supply on growth)	0.238
ϕ^{gd} (demand on growth)	0.874
$\phi^{\pi s}$ (supply on inflation)	0.376
$\phi^{\pi d}$ (demand on inflation)	0.063
κ_s (kurtosis, supply shock)	3.76
κ_d (kurtosis, demand shock)	5.63
Moments selected (of 8)	7

Notes: VAR (25) on year-over-year first-release growth and inflation; loadings and kurtoses of model (26) estimated by CMD. Residual moments are computed over the non-dummied quarters.

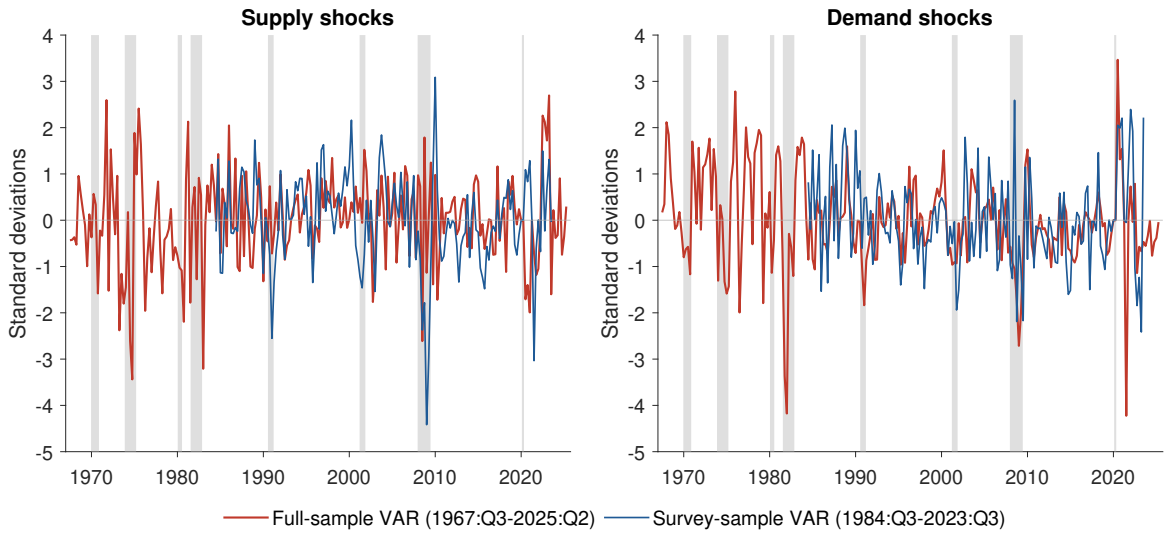

Figure C.2: Supply and demand shocks identified from realized data

Notes: Shocks from the full-sample VAR (red) and the survey-sample VAR (blue), in standard deviations. The shaded areas indicate NBER recessions.

a larger variation (0.238 vs. 0.874) in the growth residual and supply shocks account for a larger variation in the inflation residual (0.376 vs. 0.063).

Figure C.2 compares the estimates of the shock identified over the full sample and the shock identified over the survey sample. The two shocks exhibit similar patterns.

C.3 Local projections

Figure C.3 compares how forecasts respond to the belief-implied shocks and to the aggregate shocks. The responses to the belief-implied shocks come from the monthly local projection (14) in Section 4.1. Since the aggregate shocks are quarterly, I estimate the same specification on a quarterly panel:

$$y^f_{i,q+h} = \alpha_{i,h} + \beta_{s,h}\hat{u}^s_q + \beta_{d,h}\hat{u}^d_q + \mathbf{\Gamma}'_h\mathbf{X}_{iq} + e_{i,q+h} \tag{28}$$

where $y^f_{i,q}$ is forecaster i's forecast in the last month of quarter q, and $\mathbf{X}_{iq}$ contains two lags of the dependent variables and of the shocks. The estimation sample is 1984:Q4–2023:Q3. For robustness, the estimation is done using the sample period ending in 2019:Q4 to exclude the Covid period. Confidence bands are computed as in Section 4.1. Since the two sets of shocks differ in frequency, the figure plots all responses on a horizon in quarters.

The responses to the two demand shocks are similar. Growth, inflation, and interest rate forecasts all rise after a positive aggregate demand shock, as they do after a positive belief-implied demand shock. The responses to the two supply shocks differ. A positive aggregate supply shock lowers inflation forecasts, as the belief-implied supply shock does. However, a positive aggregate supply shock does not raise growth forecasts, as opposed to the common belief supply shock. One reason could be the COVID dynamics. The green line shows that the supply shock identified from the sample that excludes the period on and after 2020 raises the growth expectation. A different reason could be that the common belief supply shock's effect could be mainly due to common supply noise shock, which is also implied by the low correlation between realization-based and common belief supply shocks reported in the main text.

D Anchors and Models of Forecaster Disagreement

This section is designed to explain how the anchor term in the factor model is related to and motivated by the existing models in the literature. Recall that the empirical framework in this paper can be summarized as

$$\mathbb{F}_{it}[x_t] = b_i + \mathbb{F}^*_{it}[x_t] \tag{29}$$

where $\mathbb{F}^*_{it}[x_t]$ denotes agent i's optimal forecast for some variable x based on the most recent information and b_i indicates the deviation from $\mathbb{F}^*_{it}[x_t]$. The discussion below shows how the frameworks in Giacomini, Skreta, and Turen (2020) and Capistrán and Timmermann (2009)

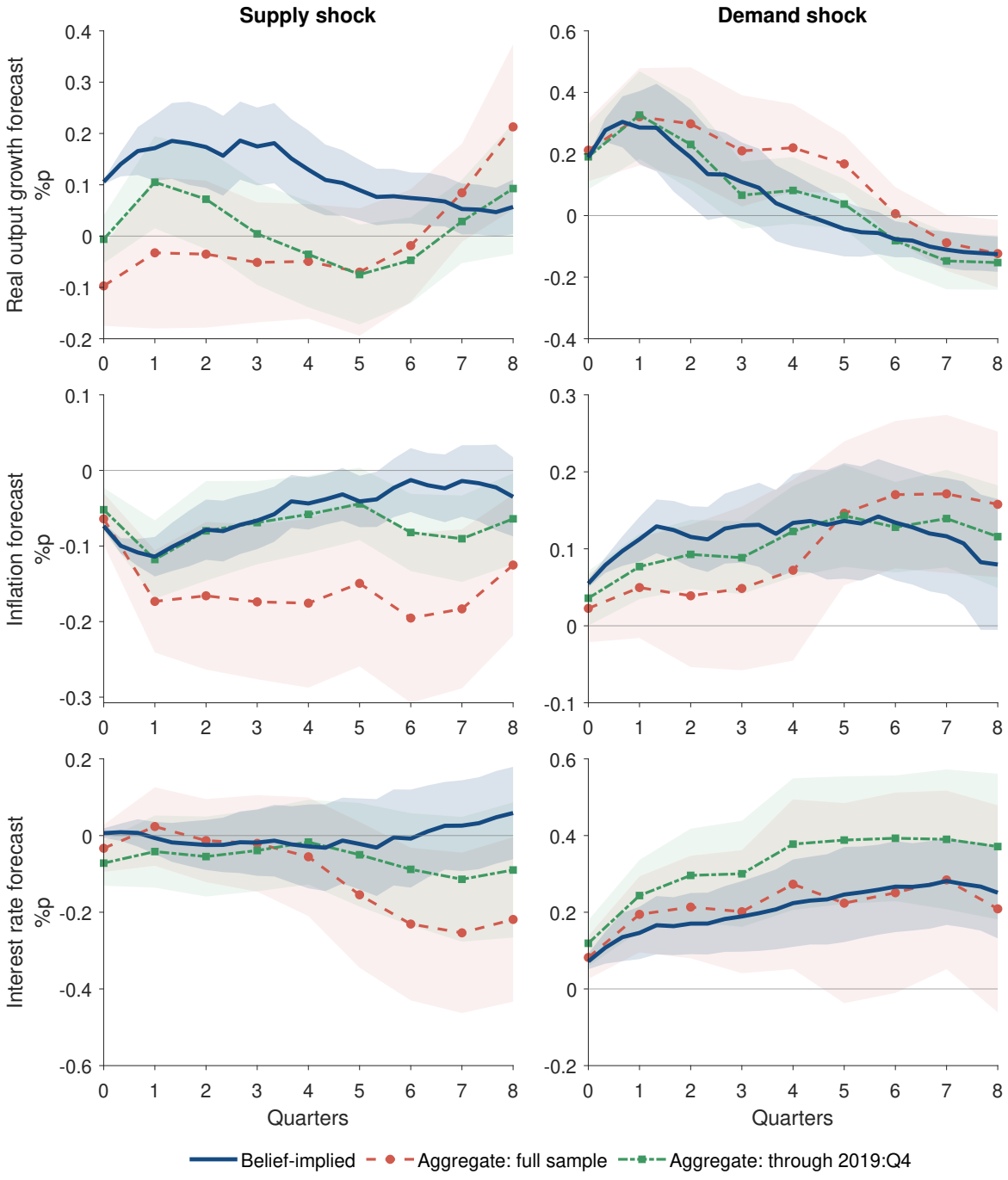

Figure C.3: Responses of forecasts to belief-implied and aggregate shocks

Notes: Belief-implied shocks: monthly local projection (14) (navy). Aggregate shocks: quarterly local projection (28) on all quarters (red, dash-dot) and through 2019:Q4 (green, dotted). Shaded areas are 90 percent confidence bands. Horizons are in quarters.

can be nested in equation (29).[28]

Heterogeneous Forecasting Models Giacomini, Skreta, and Turen (2020) propose the inclusion of a forecaster-specific intercept as a reduced-form way to capture any individual-specific source of forecast bias that can be viewed as the heterogeneity of the forecasting models. In their work, agents share a common AR(1) forecasting model for monthly inflation (x_t):

$$\mathbb{F}_{it}[x_t] = c_i + \psi x_{t-1} \tag{30}$$

In the context of this paper, $\mathbb{F}^*_{it}[x_t] = \mathbb{F}^*_t[x_t] = \psi x_{t-1}$ and $b_i = c_i$. This implies that the anchor (b_i) reflects the heterogeneity in the forecasting model.

Heterogeneous Degree of Loss Asymmetry Capistrán and Timmermann (2009) propose that agents have different asymmetric loss functions as a source of disagreement. Consider the following loss function defined on the forecast error e:

$$L_i(e;\phi_i) = \frac{1}{\phi_i^2}\Big[\exp(\phi_i e) - \phi_i e - 1\Big], \quad \phi_i \neq 0 \tag{31}$$

If $\phi_i > 0$, the loss function is almost linear for overprediction ($e < 0$) and exponential for underprediction ($e > 0$). As $\phi_i \to 0$, the loss approaches symmetric, resulting in mean-squared error loss. If the target variable is conditionally Gaussian, $x_{t|t-1} \sim \mathcal{N}(\mu_{t|t-1}, \sigma^2_{t|t-1})$, then the optimal forecast for agent i is:

$$\mathbb{F}_{it}[x_t] = \mu_{t|t-1} + \frac{\phi_i}{2}\sigma^2_{t|t-1} \tag{32}$$

The anchor in this paper would correspond to the special case where the conditional variance of the target variable is constant over time ($\sigma_{t|t-1} = \sigma$). Then, $\mathbb{F}^*_{it}[x_t] = \mu_{t|t-1}$ and $b_i = (\phi_i\sigma^2)/2$. Thus, the forecaster-specific intercept may be viewed as the heterogeneity in the loss function.

[28]The models discussed in this section assume agents have access to the history of target variables, while this paper incorporates information rigidity and agents only have access to the history of noisy signals (Clements, 2018). Nonetheless, the primary emphasis is on the motivation for introducing a bias that deviates from the optimal Bayesian forecast.

E Robustness

E.1 Interest rate forecast

The baseline analysis in the main text considers a bivariate system of forecasts, excluding the interest rate to mitigate computational challenges. Including it introduces two key complications. First, it doubles the number of parameters to be estimated per forecaster. Accounting for monetary policy shocks increases the parameter count from six (four loadings and two shock kurtoses) to twelve (nine loadings and three shock kurtoses). Second, it significantly expands the number of moment conditions. The bivariate case requires only eight, whereas incorporating interest rates raises this to 21: six second-order moments (three variances and three covariances of the growth, inflation and interest rate residuals) and fifteen fourth-order moments (three kurtoses and twelve co-kurtoses). Selecting the optimal subset of these 21 moment conditions for each forecaster presents a substantial computational burden.

To assess whether including the interest rate materially affects the baseline results, I conduct a disagreement decomposition into anchors, common belief shocks, and noise shocks using a factor model that incorporates the T-bill forecast. Three factors are chosen, as this is the point where marginal explanatory power remains significant.

The results are reported in Table E.1. While adding a third factor slightly increases the contribution of common belief shocks, the core conclusion remains robust. First, it is confirmed that noise shocks remain the primary source of disagreement across all three variables. The overall contribution is still over 60%. Second, common belief shocks contribute to growth disagreement in a counter-cyclical way, whereas the contribution to inflation is relatively more stable across the business cycle. Third, the contribution of common belief shocks is more salient in specific episodes such as the Gulf War recession. Lastly, information dispersion, as indicated by the contribution from noise shock, is a particularly important source of disagreement during the Dotcom recession.

E.2 Comparison with conventional sign restriction identification

The conventional sign restriction approach is implemented by first applying the variance operator to equation (12). This process involves the use of Cholesky decomposition, as shown below:

$$\hat{\mathbf{e}}_{it} = \mathbf{\Phi}_i \mathbf{u}_{it} \quad \Rightarrow \quad \mathbb{VAR}\left(\hat{\mathbf{e}}_{it}\right) = \mathbf{Z}_i \mathbf{Z}_i' = \mathbf{\Phi}_i \mathbf{\Phi}_i' \tag{33}$$

Table E.1: Disagreement decomposition including interest rate forecast

	Real output growth				Inflation				Interest rate			
	Sum	Anchor	Common	Noise	Sum	Anchor	Common	Noise	Sum	Anchor	Common	Noise
Full sample	100.0	24.2	13.5	62.3	100.0	13.1	22.9	64.0	100.0	21.4	13.7	64.9
Non Recession	100.0	25.3	12.5	62.2	100.0	13.4	23.3	63.4	100.0	21.9	13.4	64.7
Recession	100.0	12.2	24.5	63.3	100.0	10.1	19.0	70.9	100.0	17.1	16.7	66.2
Gulf War	100.0	14.4	40.4	45.2	100.0	6.2	28.0	65.8	100.0	44.9	10.2	44.8
Dotcom	100.0	11.9	7.5	80.6	100.0	9.8	12.7	77.5	100.0	7.8	10.0	82.2
Financial Crisis	100.0	11.1	26.4	62.5	100.0	12.8	15.8	71.5	100.0	7.2	23.3	69.5
Covid-19	100.0	14.0	15.0	71.0	100.0	5.7	31.9	62.4	100.0	24.9	13.7	61.4

Notes: Table E.1 reports the decomposition of forecast disagreement for a trivariate system that extends the baseline analysis to include short-term interest rate (T-bill) forecasts. For each variable (real output growth, inflation, and interest rate), the table presents the average percentage contributions over the specified sample period. The column "Anchor" captures the contribution from the individual fixed effect. "Common" summarizes the contribution from heterogeneous responses to common belief shocks, and "Noise" reflects the contribution from the residuals of the factor model consistent with the decomposition method in the main text.

However, it is important to note that $\mathbf{Z}_i \neq \mathbf{\Phi}_i$, primarily because $\mathbf{\Phi}_i$ is not a lower-triangular matrix and $\mathbf{Z}_i$ need not satisfy the sign restrictions. To address this, consider an orthonormal matrix $\mathbf{Q}$, satisfying $\mathbf{Q}_i\mathbf{Q}_i' = \mathbf{I}$, which leads to the following equation:

$$\mathbf{Z}_i\Big(\mathbf{Q}_i\mathbf{Q}_i'\Big)\mathbf{Z}_i' = \mathbf{\Phi}_i\mathbf{\Phi}_i' \tag{34}$$

Then, a subset of matrices $\mathbf{Q}_i$ that abide by the sign restrictions for the rotated matrix $\mathbf{Z}_i\mathbf{Q}_i$ can be identified. Given the existence of multiple feasible rotations (i.e., multiple $\mathbf{Q}_i$), the standard practice involves additional constraints, such as the signs of impulse responses up to certain horizons, or selecting $\mathbf{Q}_i$ that aligns most closely with some percentile values (e.g. median) of the distribution of rotated loadings (i.e. $\mathbf{Z}_i\mathbf{Q}_i$).

Table E.2 showcases an example where the rotation matrix $\mathbf{Q}_i$ is chosen to align its rotated loadings closely with percentile values ranging from the 40th to the 60th percentile. A key observation here is the significant impact of minor adjustments in the percentile value on the disagreement decomposition. Specifically, a rotation aligned with the 40th percentile attributes growth and inflation disagreement primarily to demand and supply noise, respectively. However, altering the benchmark to the 60th percentile reverses this interpretation, attributing growth and inflation disagreement to supply and demand noise, respectively.

Table E.2: Disagreement decomposition by using conventional sign restriction

	40th		45th		50th (Median)		55th		60th	
	SN	DN	SN	DN	SN	DN	SN	DN	SN	DN
A. Real output growth										
Full sample	28.1	42.9	31.2	39.8	34.2	36.8	37.0	34.0	39.6	31.4
Non Recession	28.3	43.2	31.4	40.0	34.4	37.1	37.2	34.3	39.9	31.6
Recession	26.3	39.8	29.3	36.8	32.1	33.9	34.9	31.2	37.5	28.6
Gulf War	22.6	23.7	24.6	21.7	26.4	19.9	28.1	18.2	29.7	16.6
Dotcom	32.9	50.5	37.3	46.1	41.3	42.1	45.2	38.2	48.8	34.6
Financial Crisis	24.6	41.9	27.3	39.1	29.9	36.5	32.5	34.0	34.9	31.6
Covid-19	28.1	43.2	32.1	39.1	36.0	35.3	39.5	31.8	43.0	28.3
1984-1999	29.8	38.9	32.6	36.1	35.3	33.4	37.9	30.8	40.3	28.4
2000-2023	27.0	45.5	30.4	42.1	33.4	39.1	36.4	36.1	39.2	33.3
B. Inflation										
Full sample	37.6	31.8	34.7	34.6	32.2	37.2	29.7	39.7	27.5	41.9
Non Recession	37.5	31.6	34.6	34.4	32.1	37.0	29.6	39.4	27.4	41.6
Recession	38.6	34.8	35.8	37.7	33.1	40.3	30.7	42.8	28.5	45.0
Gulf War	42.7	24.5	40.3	27.0	37.9	29.4	35.6	31.6	33.5	33.7
Dotcom	32.6	48.4	29.0	52.0	26.1	54.9	23.4	57.6	21.2	59.8
Financial Crisis	39.7	35.2	36.8	38.1	34.1	40.8	31.6	43.3	29.2	45.7
Covid-19	37.8	22.3	35.9	24.2	34.1	26.0	32.4	27.7	30.8	29.4
1984-1999	42.3	29.0	39.5	31.7	37.0	34.3	34.4	36.8	32.1	39.1
2000-2023	34.5	33.7	31.6	36.5	29.0	39.1	26.6	41.6	24.4	43.8

Notes: The table illustrates the noise component of disagreement decomposition using the conventional sign restriction method. Each scenario details the decomposition results based on the percentile value of the rotated loadings with which the matrix $\mathbf{Q}_i$ is most closely associated.

Table E.3: Inference on individual-optimization parameters

	$\hat{\phi}_i^{gs}$	$\hat{\phi}_i^{gd}$	$\hat{\phi}_i^{\pi s}$	$\hat{\phi}_i^{\pi d}$	$\hat{\kappa}_i^{s}$	$\hat{\kappa}_i^{d}$
1%	0.37	0.26	0.43	0.38	0.90	0.84
5%	0.72	0.71	0.70	0.77	0.94	0.96
10%	0.85	0.87	0.84	0.90	0.96	0.97

Notes: This table shows the fraction of forecasters whose parameter estimates are statistically significant. Statistical significance is determined by comparing the bootstrap distribution of parameters at each significance level with the boundary values. The boundary values for ϕ_i and κ_i are zeros and ones, respectively.

E.3 Inference

For statistical inference on the parameters being estimated from the individual CMD optimization, standard errors are computed via bootstrapping. In each bootstrap sample j, both the estimated factor model ($\mathbb{F}_{it}[\mathbf{x}_{t+h}] = \hat{\mathbf{b}}_i + \tilde{\boldsymbol{\lambda}}_i\tilde{\mathbf{f}}_t + \hat{\mathbf{v}}_{it}$) and the individual VAR model for noise ($\hat{\mathbf{v}}_{it} = \hat{\boldsymbol{\rho}}_i\hat{\mathbf{v}}_{it-1} + \hat{\boldsymbol{\Phi}}_i\hat{\mathbf{u}}_{it}$) are utilized. Specifically, for each forecaster i with N_i observations, two sets of N_i random numbers are drawn from 1 to N_i, with replacement. These random numbers are used to resample supply and demand noise shocks with replacement, generating $\mathbf{u}_{it}^{(j)}$, and reconstructing the residual term ($\hat{\mathbf{v}}_{it}^{(j)}$) using the estimated VAR model. Then, the j-th bootstrap sample for each forecaster i is defined as $\mathbb{F}_{it}^{(j)}[\mathbf{x}_{t+h}] = \hat{\mathbf{b}}_i + \tilde{\boldsymbol{\lambda}}_i\tilde{\mathbf{f}}_t + \hat{\mathbf{v}}_{it}^{(j)}$. This procedure is repeated 1,000 times, resulting in a collection of 1,000 bootstrap samples.

Table E.3 presents the results. It displays the fraction of forecasters with statistically significant estimated parameters. Statistical significance is determined based on whether the estimated parameters fall outside the confidence intervals corresponding to 1, 1.645, and 1.96 standard error bands. Notably, the findings reveal that while kurtosis estimates show relatively lower significance, more than half of the forecasters demonstrate statistically significant loading parameters, which play a crucial role in recovering supply and demand noise shocks.

In addition, Table E.4 presents the one standard error band of the disagreement decomposition from the bootstrap replications. For both output growth and inflation, the intervals indicate that the decomposition is statistically stable, and the baseline conclusions on the relative importance of each component remain robust. Wider bands are observed in short or turbulent historical episodes such as the Dotcom bubble and Covid-19, reflecting greater uncertainty, but the overall qualitative patterns remain intact.

Table E.4: Inference on disagreement decomposition

	Anchor	CS	CD	SN	DN
A. Real output growth					
Full sample	[17.7, 21.5]	[3.2, 4.8]	[4.2, 6.6]	[25.6, 31.4]	[39.5, 45.5]
Non Recession	[18.1, 22.1]	[3.0, 4.8]	[3.3, 5.8]	[26.2, 32.1]	[39.3, 45.4]
Recession	[11.3, 16.7]	[1.6, 8.4]	[11.0, 18.7]	[18.4, 25.4]	[40.5, 47.9]
Gulf War	[11.0, 23.7]	[15.7, 22.8]	[11.5, 22.6]	[15.9, 24.4]	[22.3, 30.0]
Dotcom	[7.0, 19.1]	[-6.0, -0.9]	[2.4, 11.7]	[12.9, 28.7]	[54.4, 70.8]
GFC	[8.8, 15.2]	[-1.9, 7.6]	[13.4, 23.9]	[18.1, 28.2]	[37.9, 48.8]
Covid	[12.6, 25.9]	[-4.5, 7.2]	[0.1, 16.2]	[13.6, 31.0]	[39.7, 58.3]
B. Inflation					
Full sample	[14.2, 17.3]	[4.3, 5.5]	[8.9, 11.0]	[38.6, 43.7]	[25.7, 30.8]
Non Recession	[14.7, 17.7]	[4.3, 5.6]	[8.7, 10.8]	[38.1, 43.4]	[25.7, 30.9]
Recession	[8.5, 14.1]	[1.4, 6.3]	[8.2, 14.6]	[42.2, 49.1]	[24.3, 31.3]
Gulf War	[4.4, 16.1]	[8.6, 16.0]	[5.1, 15.3]	[41.2, 51.8]	[15.8, 25.8]
Dotcom	[1.0, 12.4]	[1.3, 4.0]	[5.3, 14.0]	[34.4, 49.6]	[31.6, 46.5]
GFC	[9.0, 15.9]	[-3.8, 4.4]	[7.3, 17.5]	[43.6, 53.2]	[21.8, 31.2]
Covid	[11.7, 30.7]	[0.0, 10.2]	[2.3, 24.9]	[28.6, 45.0]	[14.7, 31.9]

Notes: Entries report one standard error range computed across bootstrap replications.

E.4 Impulse responses of macroeconomic variables

To check the dynamic relationship between macro aggregates and the identified common belief shocks, a local projection analogous to the specification in Section 4.1 is conducted as follows:

$$y_{t+h} = \alpha_h + \beta_{s,h}\hat{\epsilon}_t^s + \beta_{d,h}\hat{\epsilon}_t^d + \mathbf{\Gamma}_h'\mathbf{X}_t + e_{t+h} \tag{35}$$

In equation (35), $\hat{\epsilon}_t^s$ and $\hat{\epsilon}_t^d$ are estimated common belief supply and demand shocks. $\mathbf{X}_t$ includes six lags of shocks and dependent variables. For the dependent variable y_t, the following monthly macroeconomic variables are considered: Consumer Price Index (CPI), Industrial Production (IP), Employment (EMP), Unemployment rate (UNE), and federal funds rate (FFR).[29] CPI, IP, and EMP enter the specification in logs.

Figure E.1 presents the cumulative impulse responses $(\beta_{s,h}, \beta_{d,h})$ of each variable to a unit of positive common belief supply and demand shocks. The dark and light-shaded areas indicate 68% and 90% confidence bands. The responses are also consistent with the convention. IP and EMP increase and UNE decreases in response to both shocks. However, CPI moves in opposite directions, decreasing and increasing in response to positive supply

[29]The data are obtained from the St. Louis FRED database.

and demand shocks, respectively. As opposed to the positive response to the common belief demand shock, FFR also displays a statistically insignificant response to common belief supply shocks, reflecting the trade-off that monetary policy has to confront in response to supply shocks. Overall, the responses to the common belief supply shock are longer-lasting and persistent, which echoes the findings of Blachard and Quah (1989).

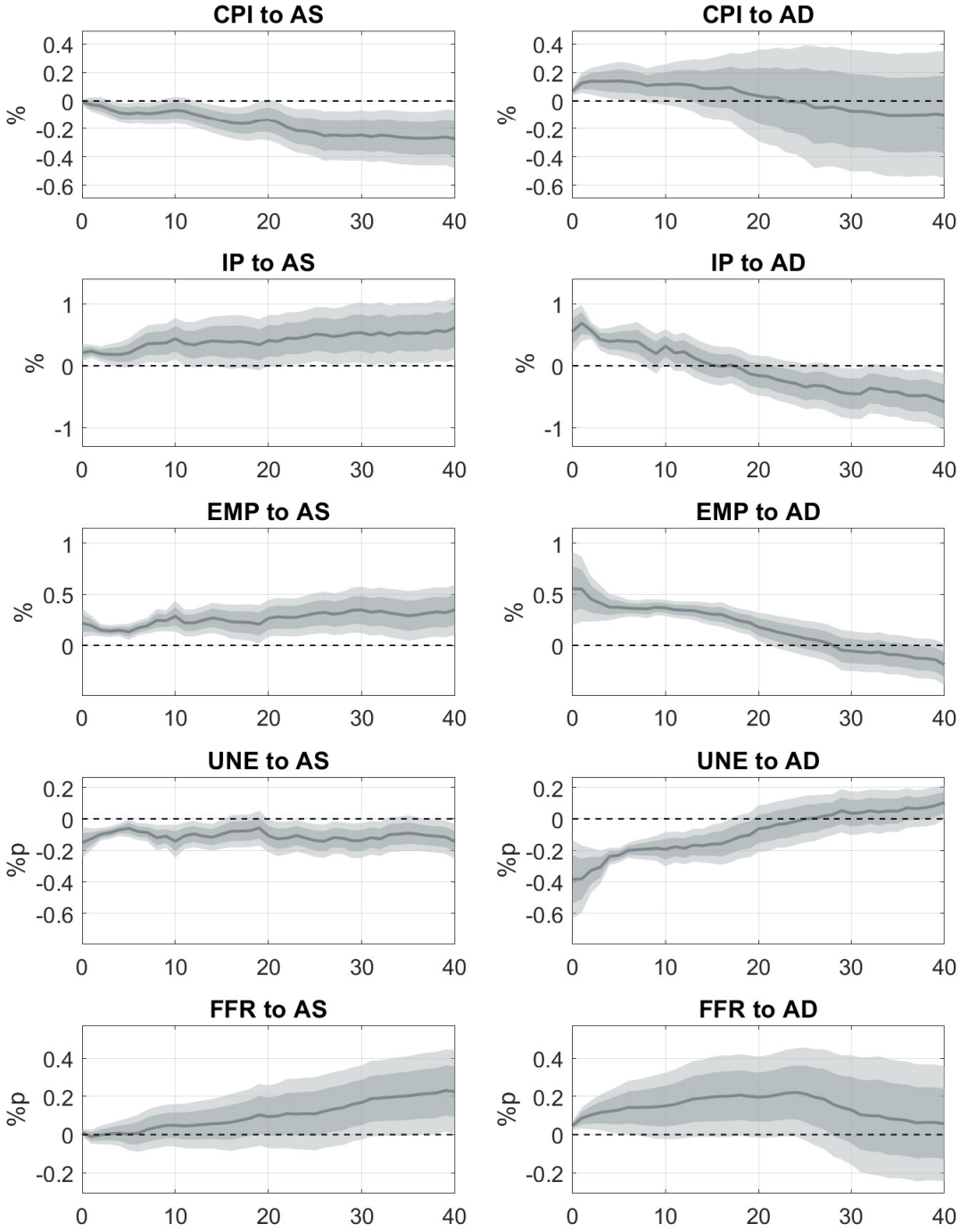

Figure E.1: Impulse Responses to Common Belief Supply and Demand Shocks.

Notes: This figure shows the impulse responses (IRFs) of macroeconomic variables to common belief supply and demand shocks. The IRFs are computed using local projection, $y_{t+h} = \alpha_h + \beta_{s,h}\hat{\epsilon}_t^s + \beta_{d,h}\hat{\epsilon}_t^d + \mathbf{\Gamma}_h'\mathbf{X}_t + e_{t+h}$. The control variables include six lags of dependent variables and shocks.

E.5 VAR lag length

Table E.5: Robustness of disagreement decomposition to VAR lag length of common factors

	VAR(2)*		VAR(3)		VAR(4)		VAR(5)	
	CS	CD	CS	CD	CS	CD	CS	CD
A. Real output growth								
Full sample	4.0	5.4	4.0	5.4	3.8	5.6	3.7	5.7
Non Recession	3.9	4.5	3.8	4.6	3.6	4.8	3.5	4.9
Recession	5.0	14.9	5.5	14.4	5.7	14.2	5.8	14.1
Gulf War	19.2	17.1	20.2	16.1	20.4	15.9	19.9	16.4
Dotcom	-3.4	7.0	-3.1	6.7	-3.2	6.8	-3.0	6.6
Financial Crisis	2.9	18.7	3.4	18.2	3.7	17.9	4.1	17.5
Covid-19	1.4	8.1	1.3	8.2	1.4	8.1	1.4	8.1
1984-1999	6.5	5.2	6.3	5.5	5.9	5.8	5.6	6.2
2000-2023	2.4	5.5	2.5	5.4	2.4	5.5	2.5	5.4
B. Inflation								
Full sample	4.9	9.9	4.9	9.9	4.7	10.1	4.6	10.2
Non Recession	5.0	9.8	5.0	9.8	4.8	10.0	4.7	10.1
Recession	3.9	11.4	4.2	11.0	4.1	11.1	4.3	11.0
Gulf War	12.3	10.2	12.7	9.8	12.7	9.8	12.1	10.4
Dotcom	2.6	9.7	3.9	8.4	2.7	9.6	3.6	8.7
Financial Crisis	0.3	12.4	0.3	12.4	0.6	12.1	0.7	11.9
Covid-19	5.1	13.6	5.0	13.7	5.1	13.6	5.3	13.4
1984-1999	8.1	6.4	8.0	6.6	7.7	6.8	7.5	7.1
2000-2023	2.8	12.2	3.0	12.1	2.8	12.3	2.8	12.2

Notes: This table presents the common belief shock component of disagreement decomposition, based on different lag lengths in a Vector Autoregression (VAR) model applied to common factors. VAR(2) represents the baseline case reported in the main text.

Table E.6: Robustness of noise shock decomposition to VAR lag length

	BIC (baseline)		AIC		VAR(1)		VAR(2)		VAR(3)	
	SN	DN	SN	DN	SN	DN	SN	DN	SN	DN
A. Real output growth										
Full sample	28.5	42.5	31.2	39.8	29.2	41.8	28.9	42.1	30.4	40.6
Non Recession	29.1	42.3	31.7	39.7	29.6	41.9	29.6	41.9	31.2	40.3
Recession	21.9	44.2	25.1	41.0	24.7	41.4	21.9	44.2	22.0	44.1
Gulf War	20.2	26.2	24.9	21.4	20.4	25.9	18.4	27.9	18.9	27.5
Dotcom	20.8	62.6	26.0	57.3	22.3	61.1	20.4	63.0	19.7	63.7
Financial Crisis	23.1	43.3	24.5	41.9	28.1	38.3	23.7	42.7	24.1	42.4
Covid-19	22.3	49.0	27.1	44.2	22.8	48.5	25.3	46.0	25.1	46.2
1984-1999	28.1	40.5	31.3	37.4	27.5	41.2	26.5	42.2	29.8	39.0
2000-2023	28.8	43.7	31.1	41.4	30.3	42.2	30.5	42.0	30.8	41.7
B. Inflation										
Full sample	41.2	28.2	38.6	30.8	41.6	27.7	41.5	27.9	40.7	28.7
Non Recession	40.8	28.3	38.3	30.8	41.3	27.8	41.2	27.9	40.2	28.8
Recession	45.7	27.8	42.8	30.6	45.9	27.5	45.1	28.3	45.2	28.2
Gulf War	46.5	20.8	39.6	27.7	44.4	22.9	47.5	19.8	44.5	22.8
Dotcom	42.0	39.0	41.4	39.6	42.3	38.7	44.3	36.7	45.8	35.2
Financial Crisis	48.4	26.5	46.7	28.2	49.5	25.4	45.5	29.4	45.1	29.8
Covid-19	36.8	23.3	32.4	27.7	38.4	21.7	37.7	22.4	46.6	13.5
1984-1999	42.0	29.2	39.3	32.0	42.5	28.7	44.5	26.8	42.3	28.9
2000-2023	40.6	27.6	38.2	29.9	41.1	27.1	39.5	28.6	39.6	28.6

Notes: This table presents the idiosyncratic shock component of disagreement decomposition, based on different lag lengths in a Vector Autoregression (VAR) model applied to idiosyncratic noise. In the main text, individual VAR lag lengths were selected based on the Bayesian Information Criterion (BIC). AIC shows the result when lag lengths were selected based on the Akaike Information Criterion. The columns labeled VAR(1) through VAR(3) represent scenarios where homogeneous lag lengths were uniformly applied to all forecasters.

E.6 Threshold

Table E.7: Contribution to Disagreement (threshold = 40)

	Sum	Anchor	C.S.	C.D.	S.N.	D.N.	Common	Noise	Supply	Demand
A. Real output growth										
Full sample	100	27.6	2.2	4.9	26.1	39.2	7.2	65.3	28.3	44.1
Non Recession	100	28.5	1.4	4.5	26.5	39.0	6.0	65.5	28.0	43.5
Recession	100	17.0	10.7	9.3	21.6	41.5	20.0	63.0	32.3	50.8
Gulf War	100	24.5	27.1	7.4	16.1	24.9	34.5	41.0	43.2	32.3
Dotcom	100	16.7	-1.1	6.9	20.4	57.1	5.8	77.5	19.2	64.0
Financial Crisis	100	13.3	9.7	11.9	24.7	40.3	21.6	65.0	34.4	52.2
Covid-19	100	18.2	3.0	5.8	21.7	51.3	8.8	73.0	24.8	57.0
1984-1999	100	35.8	2.0	3.7	24.2	34.3	5.8	58.5	26.2	38.0
2000-2023	100	22.2	2.4	5.7	27.4	42.4	8.1	69.8	29.7	48.1
B. Inflation										
Full sample	100	18.8	5.0	10.5	40.1	25.6	15.5	65.7	45.1	36.1
Non Recession	100	19.3	5.2	10.2	39.8	25.5	15.4	65.3	45.0	35.7
Recession	100	13.2	2.5	14.4	43.4	26.5	16.9	69.9	45.8	40.9
Gulf War	100	9.5	13.6	11.9	47.5	17.4	25.6	64.9	61.1	29.4
Dotcom	100	6.4	-2.6	17.1	41.0	38.1	14.5	79.1	38.4	55.2
Financial Crisis	100	17.1	-1.6	14.6	43.8	26.0	13.0	69.8	42.2	40.6
Covid-19	100	20.4	9.7	12.0	35.6	22.2	21.8	57.8	45.3	34.2
1984-1999	100	20.2	9.0	5.9	39.5	25.4	14.9	64.9	48.5	31.4
2000-2023	100	17.9	2.4	13.5	40.5	25.7	15.9	66.2	42.9	39.2

Notes: Table E.7 presents the decomposition of forecast disagreement when the minimum observation threshold per forecaster is reduced from 60 to 40.

E.7 Alternative moment conditions

Table E.8: Robustness of noise shock decomposition to moment conditions

	BIC (baseline)		AIC		HQIC	
	SN	DN	SN	DN	SN	DN
A. Real output growth						
Full sample	28.53	42.48	28.53	42.48	28.56	42.45
Non Recession	29.15	42.31	29.15	42.31	29.15	42.31
Recession	21.87	44.23	21.87	44.23	22.20	43.90
Gulf War	20.17	26.18	20.17	26.18	20.13	26.22
Dotcom	20.79	62.59	20.79	62.59	20.78	62.60
Financial Crisis	23.13	43.32	23.13	43.32	23.83	42.62
Covid-19	22.26	49.01	22.26	49.01	22.34	48.94
B. Inflation						
Full sample	41.16	28.23	41.16	28.23	41.24	28.15
Non Recession	40.75	28.27	40.75	28.27	40.84	28.17
Recession	45.66	27.78	45.66	27.78	45.57	27.87
Gulf War	46.48	20.76	46.48	20.76	46.62	20.62
Dotcom	41.98	39.02	41.98	39.02	41.80	39.20
Financial Crisis	48.41	26.48	48.41	26.48	47.96	26.93
Covid-19	36.78	23.34	36.78	23.34	38.53	21.59

Notes: Table E.8 compares the noise shock component of disagreement decomposition result based on alternative moment selection criteria of Andrews and Lu (2001). Results are shown using three different criteria for selecting the optimal set of moment conditions: the BIC, which is the baseline criterion used in the main text, the AIC, and the HQIC. The moment selection criteria can be found in Appendix B.3.

E.8 Different number of factors

Table E.9: Disagreement decomposition with an additional factor

	Real output growth				Inflation			
	Sum	Anchor	Common	Noise	Sum	Anchor	Common	Noise
Three factors								
Full sample	100.0	18.4	20.5	61.1	100.0	21.2	16.7	62.2
Non Recession	100.0	18.6	20.0	61.4	100.0	21.6	16.7	61.7
Recession	100.0	15.8	26.0	58.3	100.0	16.1	16.9	67.1
Gulf War	100.0	11.3	42.5	46.2	100.0	16.6	17.9	65.5
Dotcom	100.0	8.6	17.2	74.2	100.0	3.8	22.4	73.8
Financial Crisis	100.0	18.7	24.3	57.0	100.0	19.9	12.9	67.3
Covid-19	100.0	32.0	13.3	54.7	100.0	27.1	22.4	50.5

Notes: The table shows the disagreement decomposition when estimating the model with three common factors (baseline: two factors).